Research in Physics 2008-2013

Centre for Fusion Space and Astrophysics (CFSA)

- *9 Staff; 7 PDRAs; 26 PhDs;*
- *251 articles; 2375 citations; £6.3 M grant awards; ~£1 M in-kind; 22 PhDs awarded*









CFSA is one of the largest interdisciplinary plasma physics centres in Europe. Its mission is to address key physics questions that arise from the grand challenges of fusion energy and the solar-terrestrial environment, and that require deep expertise in plasma physics to solve. The twin-track approach of contributing to fundamental physics and mission-led programmes ensures CFSA's activity is relevant to diverse funding sources: EPSRC/STFC, Euratom/ESA, and aligns with the UK's strategic energy and environmental needs. The group has a strong international reputation that is sustained through close partnerships with large facilities and their communities. These incl. Euratom magnetic confinement fusion (JET, MAST) at Culham & LHD, Japan (**Chapman**, **Dendy**, **Hnat**, **McMillan**, **Verwichte**); laser-driven fusion at RAL and AWE (**Arber**, **Gericke**); ground & satellite observatories for the solar corona (**Broomhall**, **Nakariakov**, **Verwichte**) and for the solar wind and Earth's magnetosphere (**Chapman**, **Hnat**). Extensive research partnerships include university level agreements with U. Kyushu and the Mexican Science Research Agency.

CFSA plays a major role in providing research training for energy and space environment missions and is a founding member of the European Fusion Education Association (FUSENET). There is a steady flow of overseas PhD students with their own funding for both fusion and solar-terrestrial plasma research and 24 PhD students have been co-supervised with staff at Culham, RAL and AWE.

Solar wind turbulence ranks amongst the most important research topics in plasma astrophysics[1] and has been identified by international space agencies[†] as a scientific question to be addressed with future spacecraft. CFSA will continue to lead in the analysis of data from ESA- and NASA-led solar wind missions that span latitude and distance (ULYSSES), cover several solar cycles (WIND, ACE), and are at high cadence (**Chapman** is Co-I on CLUSTER). The Group's novel data analysis methodology means it will be a core science partner in future international missions, incl. Deep Space Climate

1 Princeton WOPA report, 2011

†ESA Cosmic Vision; NRC Decadal Strategy for Solar and Space Physics 2013-2022 (NASA); JAXA Vision 2025

Observatory (launch: 2014); ESA Solar Orbiter (2017), and NASA-led Magneto-spheric Multi-Scale and Solar Probe Plus (2018).

As an international leader in wave processes in coronal plasmas, **Nakariakov** will use his ERC Advanced Grant SeismoSun to exploit solar MHD seismology data from spacecraft (SDO, Hinode, STEREO) and be in the science teams of future space & ground-based projects (ESA Solar Orbiter, ALMA).

With the latest *high-power laser systems* [ELI, Vulcan, HERCULES, LCLS free electron laser] entering new plasma regimes, CFSA are leading theory support for high-energy-density matter experiments (**Gericke**) and at the forefront of world QED-plasma research through development of the EPOCH-QED code (**Arber**).

Laser Absorption in Relativistically Underdense Plasmas by Synchrotron Radiation

Physical Review Letters, 109, 245006 (2012) DOI: http://dx.doi.org/10.1103/PhysRevLett.109.245006

C. S. Brady, C. P. Ridgers, T. D. Arber, A. R. Bell, and J. G. Kirk

A novel absorption mechanism for linearly polarized lasers propagating in relativistically under-dense solids in the ultra-relativistic (a ! 100) regime is presented. The mechanism is based on strong synchrotron emission from electrons re-injected into the laser by the space charge field they generate at the front of the laser pulse. This laser absorption, termed re-injected electron synchrotron emission, is due to a coupling of conventional plasma physics processes to quantum electrodynamic processes in low density solids at intensities above 1022 W=cm^2. Re-injected electron synchrotron emission is identified in 2D QED-particle-in-cell simulations and then explained in terms of 1D QED-particle-in-cell simulations and simple analytical theory. It is found that between 1% (at 1022 W=cm^2) and 14% (at 8 " 1023 W=cm^2) of the laser energy is converted into gamma ray photons, potentially providing an ultra-intense future gamma ray source.

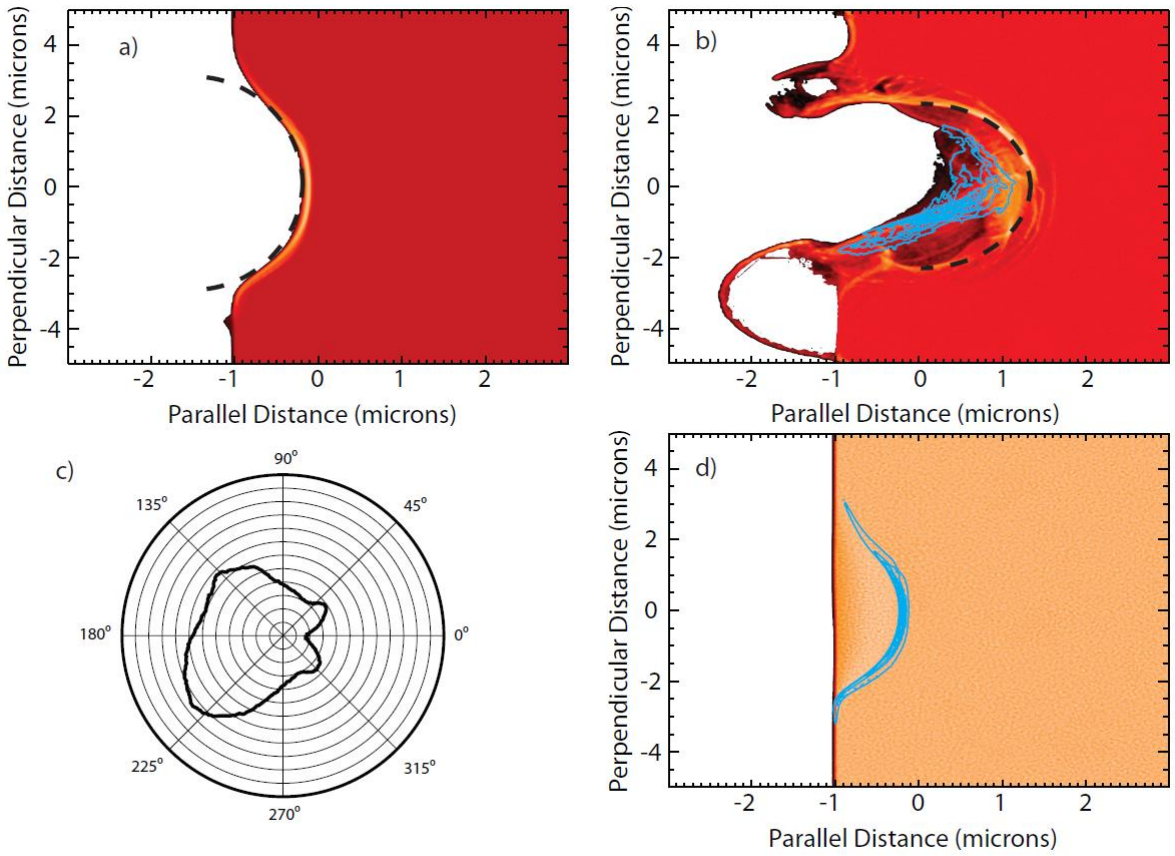

Dense Electron-Positron Plasmas and Ultra-Intense Gamma-Rays from Laser-Irradiated Solids

Physical Review Letters 108 (16) , art. no. 165006 (2012) DOI: doi:10.1103/PhysRevLett.108.165006

C.P. Ridgers, C.S. Brady, R. Duclous, J.G. Kirk, K. Bennett, T.D. Arber, A.P.L. Robinson, A.R. Bell

In simulations of a 10 PW laser striking a solid, we demonstrate the possibility of producing a pure electron-positron plasma by the same processes as those thought to operate in high-energy astrophysical environments. A maximum positron density of 10^{26} m^{-3} can be achieved, 7 orders of magnitude greater than achieved in previous experiments. Additionally, 35% of the laser energy is converted to a burst of γ rays of intensity 10^{22} $W\,cm^{-2}$, potentially the most intense γ-ray source available in the laboratory. This absorption results in a strong feedback between both pair and γ-ray production and classical plasma physics in the new "QED-plasma" regime.

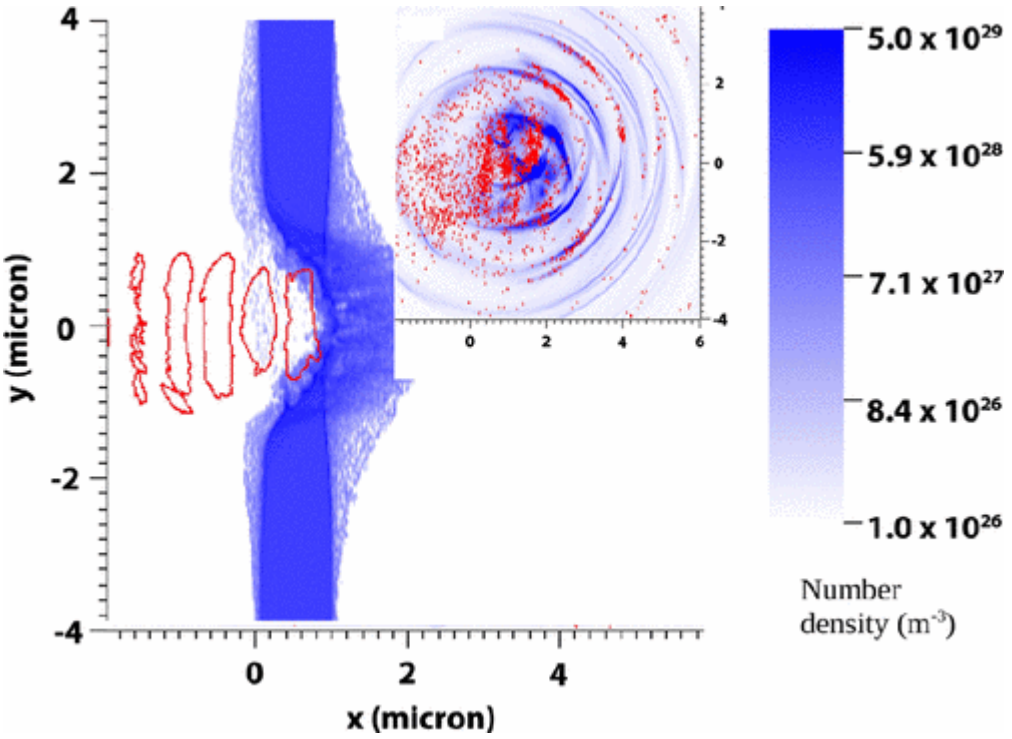

Pair production by a laser of intensity 4×10^{23} W cm^{-2} striking an aluminum target (snapshots at the end of the 30 fs laser pulse). The laser (red contours) bores a hole into the solid target (blue density map). *γ* rays (blue density map) and positrons (red dots) are generated in this interaction (inset—on the same scale).

Effect of solar chromospheric neutrals on equilibrium field structures

Astrophysical Journal Letters 705 (2) , pp. 1183-1188 (2009) doi:10.1088/0004-637X/705/2/1183

T. D. Arber, G. J. J. Botha and C. S. Brady

Solar coronal equilibrium fields are often constructed by nonlinear force-free field (NLFFF) extrapolation from photospheric magnetograms. It is well known that the photospheric field is not force-free and the correct lower boundary for NLFFF construction ought to be the top of the chromosphere. To compensate for this, pre-filtering algorithms are often applied to the photospheric data to remove the non-force-free components. Such pre-filtering models, while physically constrained, do not address the mechanisms that may be responsible for the field becoming force-free. The chromospheric field can change through, for example, field expansion due to gravitational stratification, reconnection, or flux emergence. In this paper, we study and quantify the effect of the chromospheric neutrals on equilibrium field structures. It is shown that, depending on the degree to which the photospheric field is not force-free, the chromosphere will change the structure of the equilibrium field. This is quantified to give an estimate of the change in α profiles one might expect due to neutrals in the chromosphere. Simple scaling of the decay time of non-force-free components of the magnetic field due to chromospheric neutrals is also derived. This is used to quantify the rate at which, or equivalent at which height, the chromosphere is expected to become force-free.

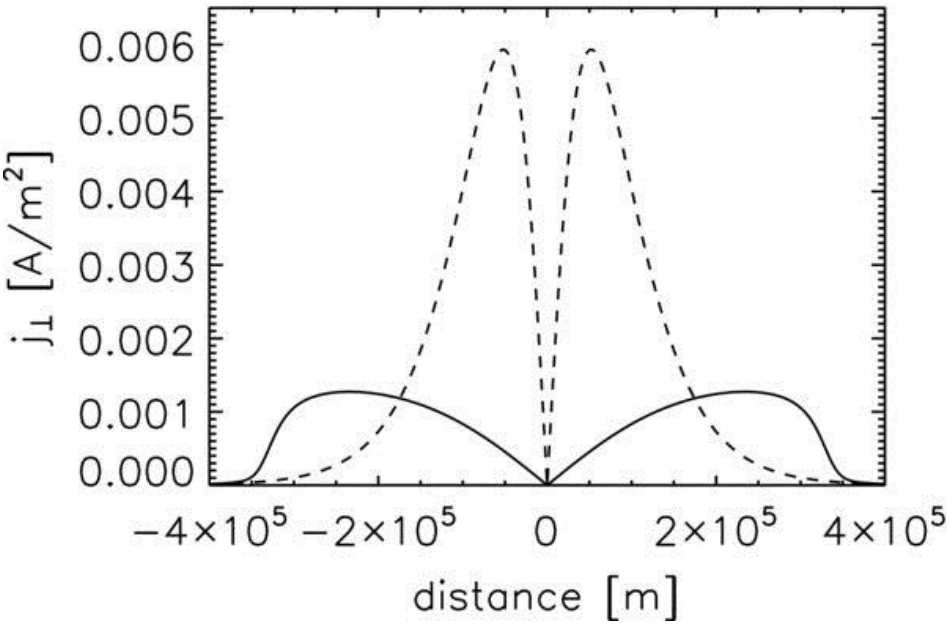

Profiles of $j_\perp$ at 1000 s (solid line) and at t = 0 (broken line) obtained with $\eta_\perp$ = 61.86 m^2 s^{-1} and b = 0.5 in Equation (10).

Chromospheric Resonances Above Sunspot Umbrae

Astrophysical Journal Letters 728 (2) 84-91 (2011) doi:10.1088/0004-637X/728/2/84

G. J. J. Botha, T. D. Arber, V. M. Nakariakov, and Y. D. Zhugzhda

Three-minute oscillations are observed in the chromosphere above sunspot umbrae. One of the models used to explain these oscillations is that of a chromospheric acoustic resonator, where the cavity between the photosphere and transition region partially reflects slow magnetoacoustic waves to form resonances in the lower sunspot atmosphere. We present a phenomenological study that compares simulation results with observations. The ideal magnetohydrodynamic equations are used with a uniform vertical magnetic field and a temperature profile that models sunspot atmospheres above umbrae. The simulations are initialized with a single broadband pulse in the vertical velocity inside the convection zone underneath the photosphere. The frequencies in the spectrum of the broadband pulse that lie below the acoustic cutoff frequency are filtered out so that frequencies equal and above the acoustic cutoff frequency resonate inside the chromospheric cavity. The chromospheric cavity resonates with approximately three-minute oscillations and is a leaky resonator, so that these oscillations generate traveling waves that propagate upward into the corona. Thus, there is no requirement that a narrowband three-minute signal is present in the photosphere to explain the narrowband three-minute oscillations in the chromosphere and corona. The oscillations in the chromospheric cavity have larger relative amplitudes (normalized to the local sound speed) than those in the corona and reproduce the intensity fluctuations of observations. Different umbral temperature profiles lead to different peaks in the spectrum of the resonating chromospheric cavity, which can explain the frequency shift in sunspot oscillations over the solar cycle.

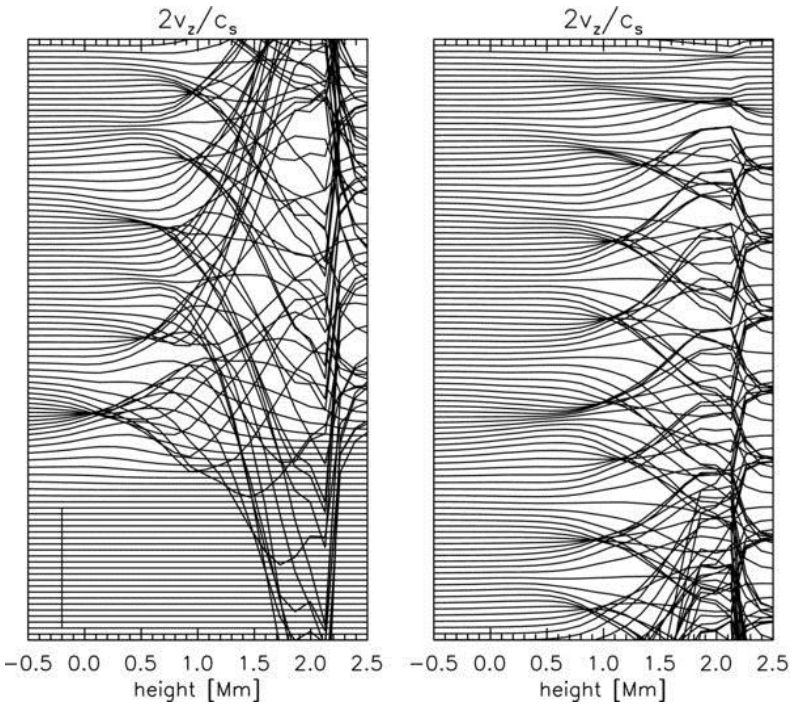

Resonances in the chromospheric cavity. The amplitude of $2v_z/c_s$ is plotted against height, with v_z the vertical velocity and c_s the local sound speed. The vertical line in the bottom left-hand corner shows the scale of an amplitude of 10^{-2}. Every 18 s a profile is plotted, shifted up from the previous profile. The figure on the left-hand side starts at initialization at the bottom and ends at time 1800 s at the top. The figure on the right continues at time 1800 s at the bottom and ends at time 3600 s at the top.

Ensemble asteroseismology of solar-type stars with the NASA kepler mission

Science, 332, 213-216 (2011) DOI: 10.1126/science.1201827

Chaplin, W.J., *et al.* incl A-M Broomhall

In addition to its search for extrasolar planets, the NASA Kepler mission provides exquisite data on stellar oscillations. We report the detections of oscillations in 500 solar-type stars in the Kepler field of view, an ensemble that is large enough to allow statistical studies of intrinsic stellar properties (such as mass, radius, and age) and to test theories of stellar evolution. We find that the distribution of observed masses of these stars shows intriguing differences to predictions from models of synthetic stellar populations in the Galaxy.

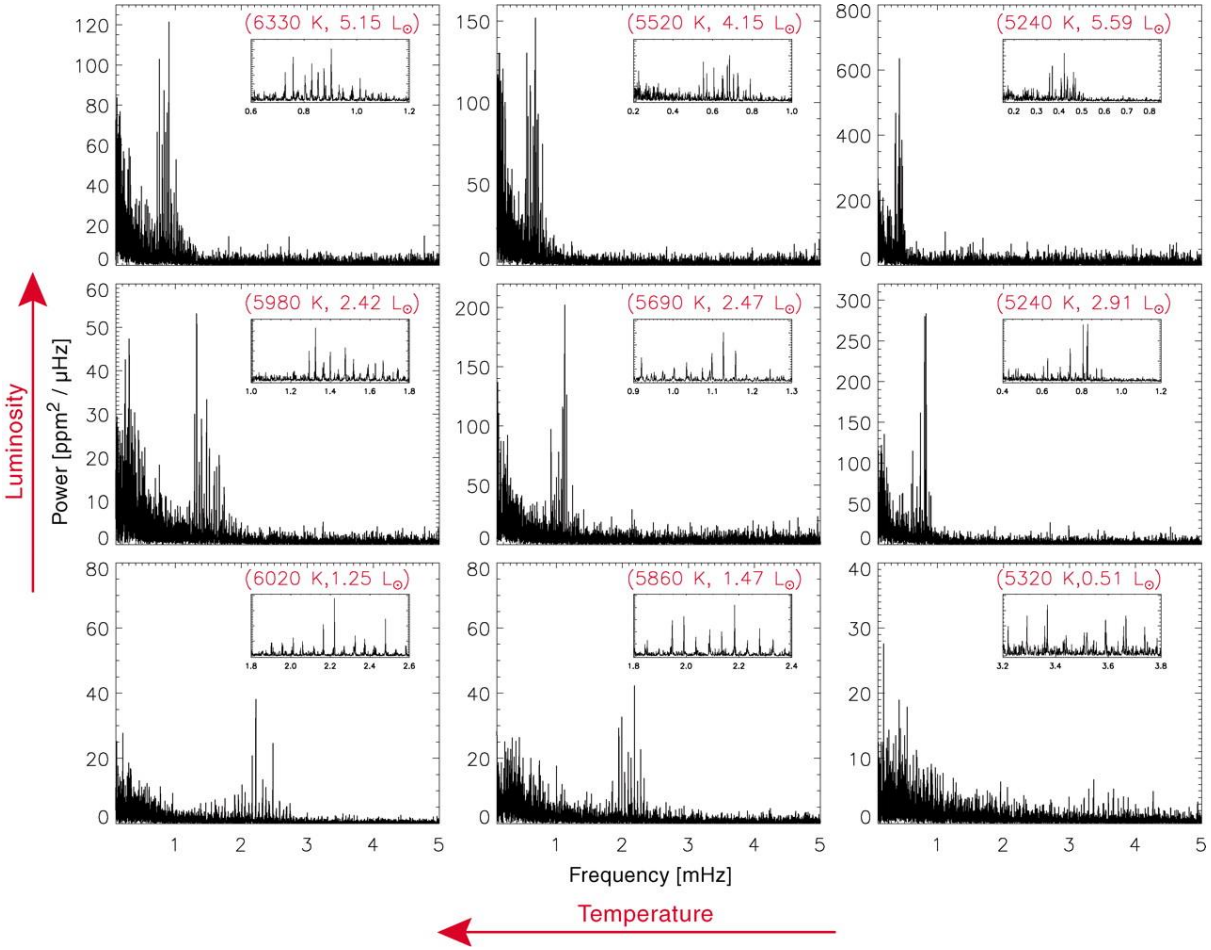

Frequency spectra of the oscillations exhibited by nine stars from the ensemble. Each spectrum shows a prominent Gaussian-shaped excess of power because of the oscillations, centered on the frequency ν_{max}. (**Insets**) Clearer views of the near-regular spacings in frequency between individual modes of oscillation within each spectrum. The stars are arranged by intrinsic brightness [in units of solar luminosity ($L_\odot$)] and temperature, with intrinsically fainter stars showing weaker, less prominent oscillations than their intrinsically brighter cousins. ppm, parts per million.

Gravity modes as a way to distinguish between hydrogen- and helium-burning red giant stars

Nature, 471, 608-611 (2011) doi:10.1038/nature09935

Bedding, T.R., *et al.* incl A-M Broomhall

Red giants are evolved stars that have exhausted the supply of hydrogen in their cores and insteadburn hydrogen in a surrounding shell. Once a red giant is sufficiently evolved, the helium in the core also undergoes fusion. Outstanding issues in our understanding of red giants include uncertainties in the amount ofmass lost at the surface before helium ignition and the amount of internal mixing fromrotation and other processes. Progress is hampered by our inability to distinguish between red giants burning helium in the core and those still only burning hydrogen in a shell.Asteroseismology offers a way forward, being a powerful tool for probing the internal structures of stars using their natural oscillation frequencies. Here we report observations of gravity-mode period spacings in red giants that permit a distinction between evolutionary stages to be made. We use high-precision photometry obtained by the Kepler spacecraft over more than a year to measure oscillations in several hundred red giants.We findmany stars whose dipole modes show sequences with approximately regular period spacings. These stars fall into two clear groups, allowing us to distinguish unambiguously between hydrogen- shell-burning stars (period spacing mostly 50 seconds) and those that are also burning helium (period spacing 100 to 300 seconds).

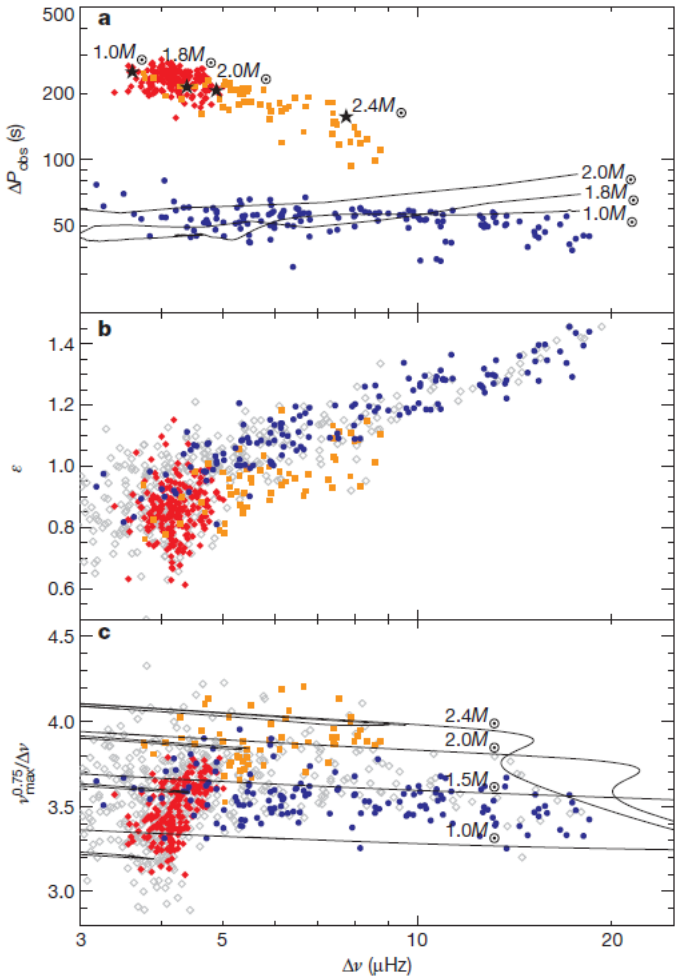

Asteroseismic diagrams for red giants observed with Kepler. Theabscissa is the p-mode large frequency separation.

Is the current lack of solar activity only skin deep?

Astrophysical Journal Letters, 700, L162-165 (2010) doi:10.1088/0004-637X/700/2/L162

Broomhall, A.-M., Chaplin, W.J., Elsworth, Y., Fletcher, S.T., New, R.

The Sun is a variable star whose magnetic activity and total irradiance vary on a timescale of approximately 11 years. The current activity minimum has attracted considerable interest because of its unusual duration and depth. This raises the question: what might be happening beneath the surface where the magnetic activity ultimately originates? The surface activity can be linked to the conditions in the solar interior by the observation and analysis of the frequencies of the Sun's natural seismic modes of oscillation—the p modes. These seismic frequencies respond to changes in activity and are probes of conditions within the Sun. The Birmingham Solar-Oscillations Network (BiSON) has made measurements of p-mode frequencies over the last three solar activity cycles, and so is in a unique position to explore the current unusual and extended solar minimum. We show that the BiSON data reveal significant variations of the p-mode frequencies during the current minimum. This is in marked contrast to the surface activity observations, which show little variation over the same period. The level of the minimum is significantly deeper in the p-mode frequencies than in the surface observations. We observe a quasi-biennial signal in the p-mode frequencies, which has not previously been observed at mid- and low-activity levels. The stark differences in the behavior of the frequencies and the surface activity measures point to activity-related processes occurring in the solar interior, which are yet to reach the surface, where they may be attenuated.

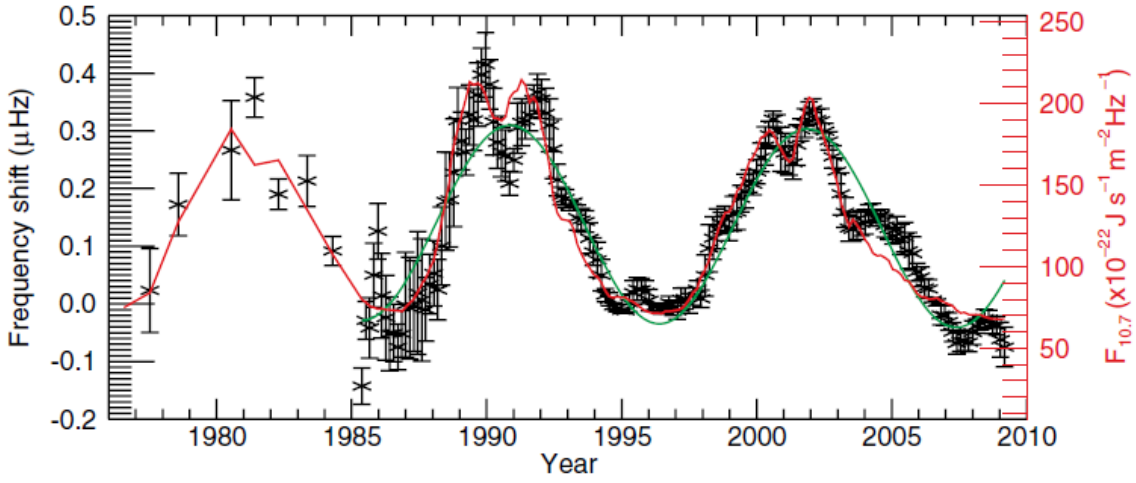

Smoothed frequency shifts observed in BiSON data during cycles 21, 22, and 23. The error bars associated with the frequency-shift data are due to uncertainties in the fitted oscillation frequencies. The green line is a sinusoid which has been fitted to the seismic data. Overplotted in red, and using the right-hand axis, is the $F_{10.7}$, which has been scaled using a linear fit to the observed frequency shifts.

Global Scale-Invariant Dissipation in Collisionless Plasma Turbulence

Phys. Rev. Lett., 103, 075006 (2009) DOI: http://dx.doi.org/10.1103/PhysRevLett.103.075006

K. H. Kiyani, S. C. Chapman, Yu. V. Khotyaintsev, M. W. Dunlop, F. Sahraoui

A higher-order multiscale analysis of the dissipation range of collisionless plasma turbulence is presented using *in situ* high-frequency magnetic field measurements from the Cluster spacecraft in a stationary interval of fast ambient solar wind. The observations, spanning five decades in temporal scales, show a crossover from multifractal intermittent turbulence in the inertial range to non-Gaussian monoscaling in the dissipation range. This presents a strong observational constraint on theories of dissipation mechanisms in turbulent collisionless plasmas.

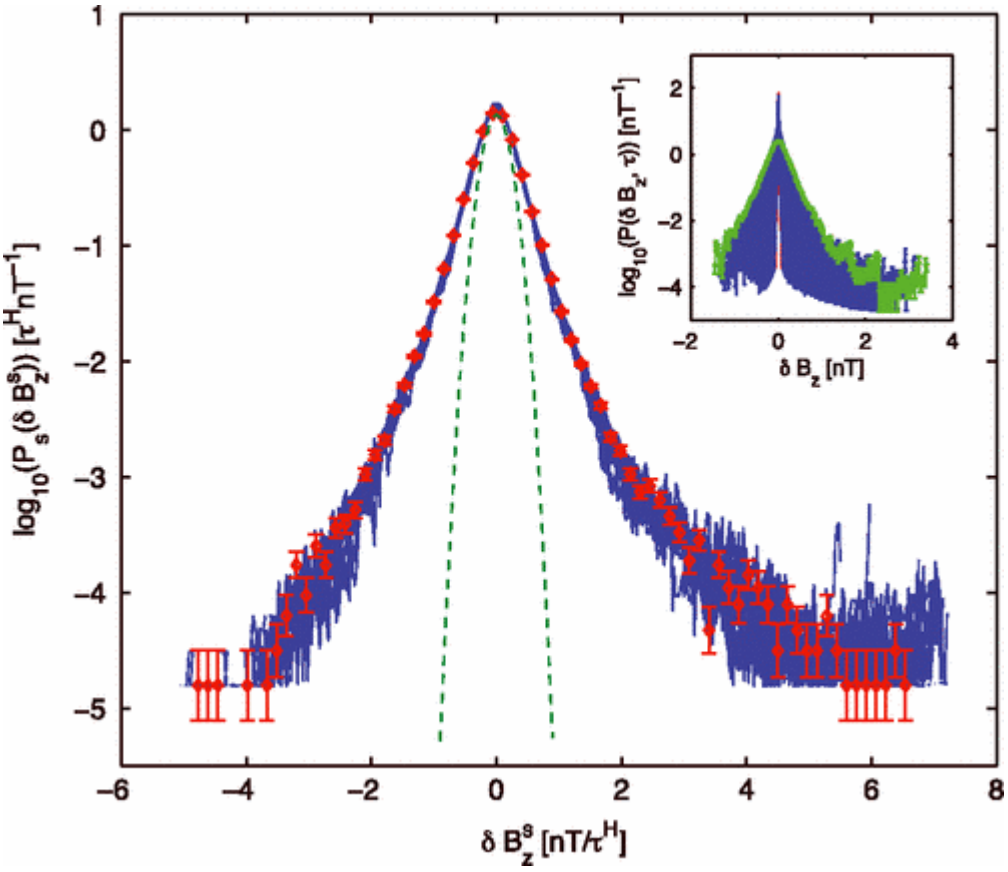

Main plot: PDFs rescaled using Eq. (3) ($\delta B_z^s = \delta B_z \tau^{-H}$). A Gaussian fit to the data (dashed curve) illustrates the heavy-tailed non-Gaussian nature of the rescaled PDF. Inset: PDFs at different scales τ before rescaling; inner and outermost curves show the smallest and largest values of τ, respectively.

Generalized Similarity in Finite Range Solar Wind Magnetohydrodynamic Turbulence

*Phys. Rev. Lett.,*103, 241101, (2009) DOI: http://dx.doi.org/10.1103/PhysRevLett.103.241101

S. C. Chapman, R. M. Nicol

Extended or generalized similarity is a ubiquitous but not well understood feature of turbulence that is realized over a finite range of scales. The ULYSSES spacecraft solar polar passes at solar minimum provide *in situ* observations of evolving anisotropic magnetohydrodynamic turbulence in the solar wind under ideal conditions of fast quiet flow. We find a single generalized scaling function characterizes this finite range turbulence and is insensitive to plasma conditions. The recent unusually inactive solar minimum—with turbulent fluctuations down by a factor of ~2 in power—provides a test of this invariance.

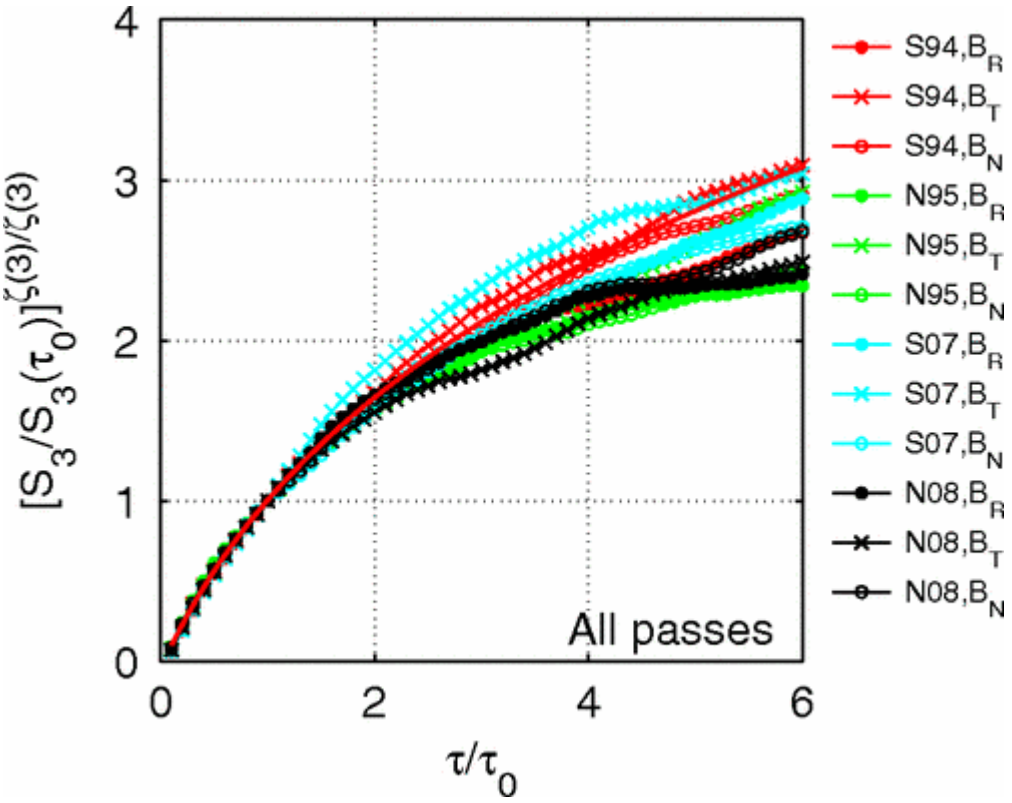

$[S_3(\tau)/S_3(\tau_0)]^{\zeta(3)/\zeta(3)}$ versus τ/τ_0 for all field components for 10 d intervals at the same heliocentric distance for each of the ULYSSES polar passes: south 1994 (days 260–269), north 1995 (days 240–249), south 2007 (days 60–69) and north 2008 (days 40–49).

Identifcation of intermittent multi-fractal turbulence in fully kinetic simulations of magnetic reconnection

Phys. Rev. Lett. 110, 205002 (2013) DOI: http://dx.doi.org/10.1103/PhysRevLett.110.205002

E. Leonardis, S. C. Chapman, W. Daughton, V. Roytershteyn, and H. Karimabadi

Recent fully nonlinear, kinetic three-dimensional simulations of magnetic reconnection [W. Daughton *et al.*, Nat. Phys. **7**, 539 (2011)] evolve structures and exhibit dynamics on multiple scales, in a manner reminiscent of turbulence. These simulations of reconnection are among the first to be performed at sufficient spatiotemporal resolution to allow formal quantitative analysis of statistical scaling, which we present here. We find that the magnetic field fluctuations generated by reconnection are anisotropic, have nontrivial spatial correlation, and exhibit the hallmarks of finite range fluid turbulence: they have non-Gaussian distributions, exhibit extended self-similarity in their scaling, and are spatially multifractal. Furthermore, we find that the rate at which the fields do work on the particles, **J.E**, is also multifractal, so that magnetic energy is converted to plasma kinetic energy in a manner that is spatially intermittent. This suggests that dissipation in this sense in collisionless reconnection on kinetic scales has an analogue in fluidlike turbulent phenomenology, in that it proceeds via multifractal structures generated by an intermittent cascade.

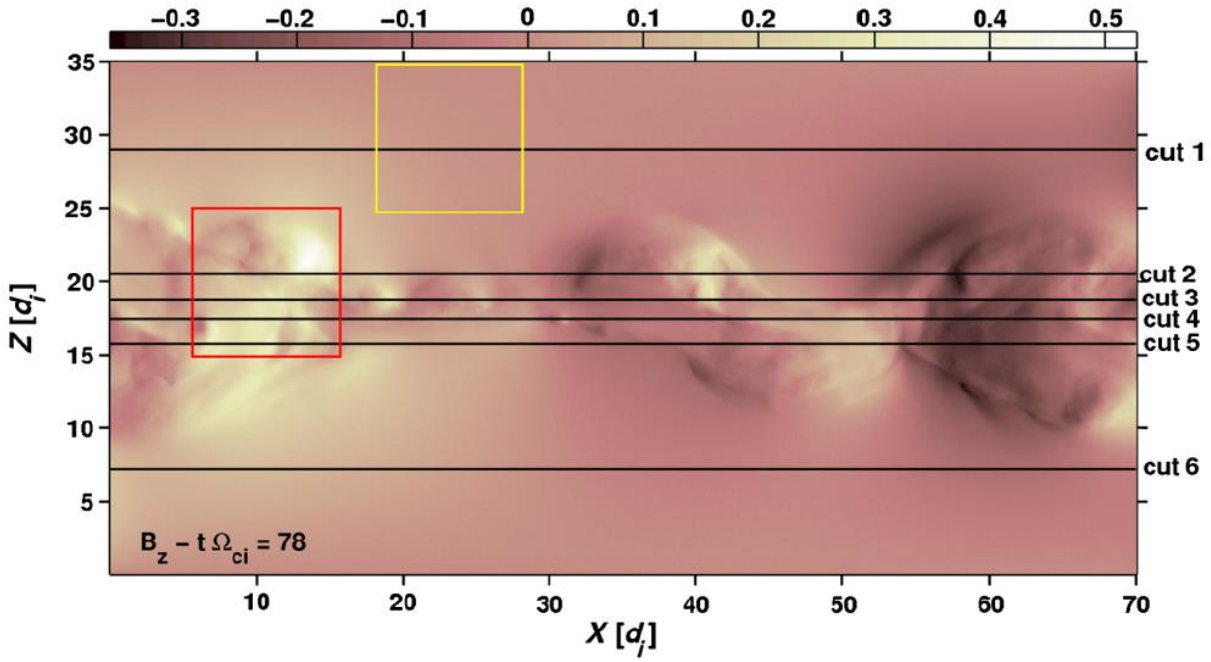

B_z in the X-Z plane at Y = 35d_i and at the time tΩ_{ci} = 78 of the simulation. Solid black lines are the cuts chosen for the analysis of the magnetic fluctuations, while squares indicate the regions over which we perform the boxcounting analysis of **J.E**.

Nonaxisymmetric anisotropy of solar wind turbulence as a direct test for models of magnetohydrodynamic turbulence

Phys. Rev. Lett., 108, 085001, (2012) DOI: http://dx.doi.org/10.1103/PhysRevLett.108.085001v

A. J. Turner, G. Gogoberidze, S. C. Chapman

Single point spacecraft observations of the turbulent solar wind flow exhibit a characteristic nonaxisymmetric anisotropy that depends sensitively on the perpendicular power spectral exponent. We use this nonaxisymmetric anisotropy as a function of wave vector direction to test models of MHD turbulence. Using Ulysses magnetic field observations in the fast, quiet polar solar wind we find that the Goldreich-Sridhar model of MHD turbulence is not consistent with the observed anisotropy, whereas the observations are well reproduced by the "slab+2D" model. The Goldreich-Sridhar model alone cannot account for the observations unless an additional component is also present.

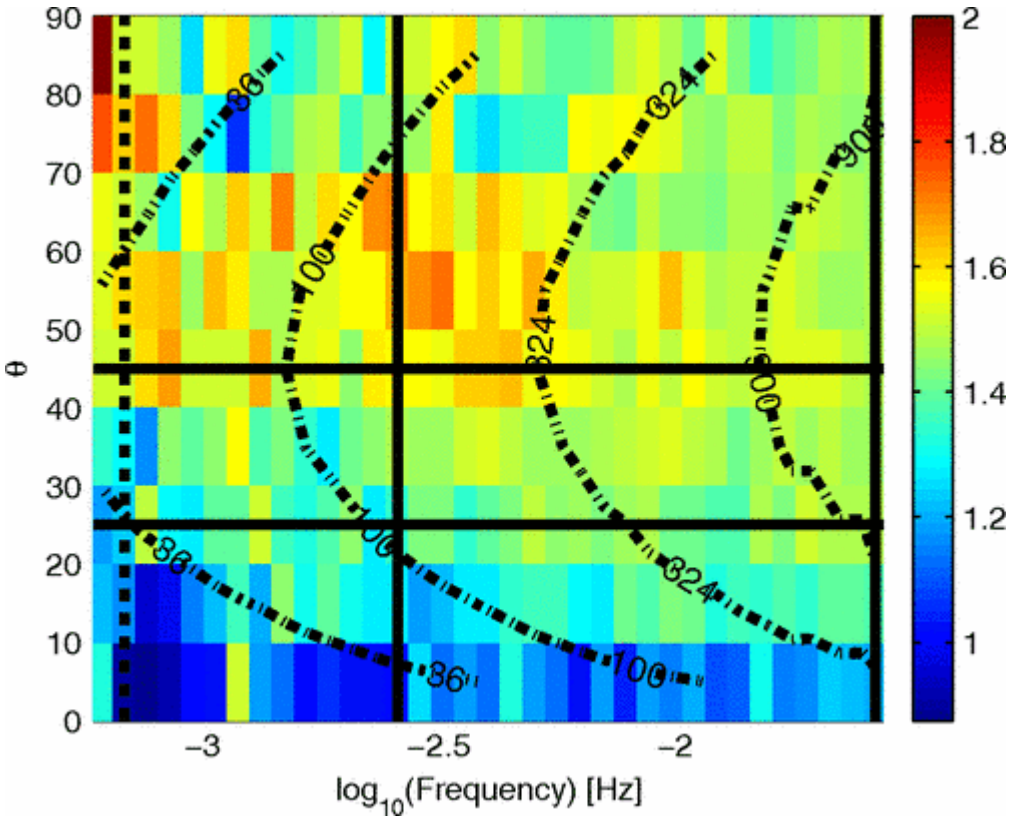

The surface $R(\vartheta,f)$ is shown in color. The black solid lines indicate the cuts of $R(\vartheta,f)$ shown in Fig. 1. The dashed line shows the start of the inertial range, F=1. The dash-dotted lines show contours of subinterval sample size. The number of samples in the interval is indicated on the contours. The color bar shows the ratio $R(\vartheta,f)=\tilde{P}_{xx}(\vartheta,f)/\tilde{P}_{xx}(\vartheta,f)$

Electron Current Drive by Fusion-Product-Excited Lower Hybrid Drift Instability

Phys. Rev. Lett. 105, 255003 (2010) DOI: http://dx.doi.org/10.1103/PhysRevLett.105.255003

J. W. S. Cook, S. C. Chapman, R. O. Dendy

We present first principles simulations of the direct collisionless coupling of the free energy of fusion-born ions into electron current in a magnetically confined fusion plasma. These simulations demonstrate, for the first time, a key building block of some “alpha channeling” scenarios for tokamak experiments. Spontaneously excited obliquely propagating waves in the lower hybrid frequency range undergo Landau damping on resonant electrons, drawing out an asymmetric tail in the electron parallel velocity distribution, which carries a current.

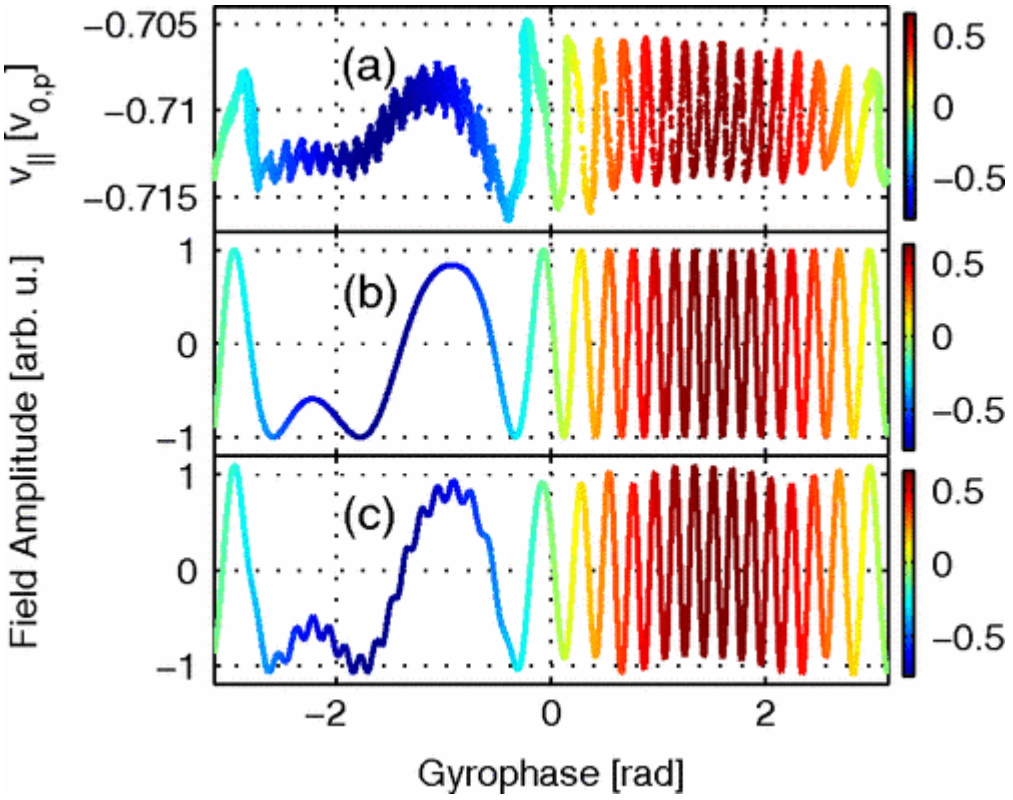

Panel (a) Snapshot at time (iii) of the energetic proton velocity space. Velocity space coordinates are $v_{\|}$ (abscissa), gyrophase (ordinate), and v_x (shading).

Panel (b) Normalized wave amplitude seen by protons at resonance with the dominant wave plotted as a function of phase space.

Panel (c) As in panel (b) for a sum of dominant wave mode and the counterpropagating damped mode

Statistical Characterization and Classification of Edge-Localized Plasma Instabilities

Phys. Rev. Lett. 110, 155004 (2013) DOI: http://dx.doi.org/10.1103/PhysRevLett.110.155004

A. J. Webster and R. O. Dendy

The statistics of edge-localized plasma instabilities (ELMs) in toroidal magnetically confined fusion plasmas are considered. From first principles, standard experimentally motivated assumptions are shown to determine a specific probability distribution for the waiting times between ELMs: the Weibull distribution. This is confirmed empirically by a statistically rigorous comparison with a large data set from the Joint European Torus. The successful characterization of ELM waiting times enables future work to progress in various ways. Here we present a quantitative classification of ELM types, complementary to phenomenological approaches. It also informs us about the nature of ELM processes, such as whether they are random or deterministic. The methods are extremely general and can be applied to numerous other quasiperiodic intermittent phenomena.

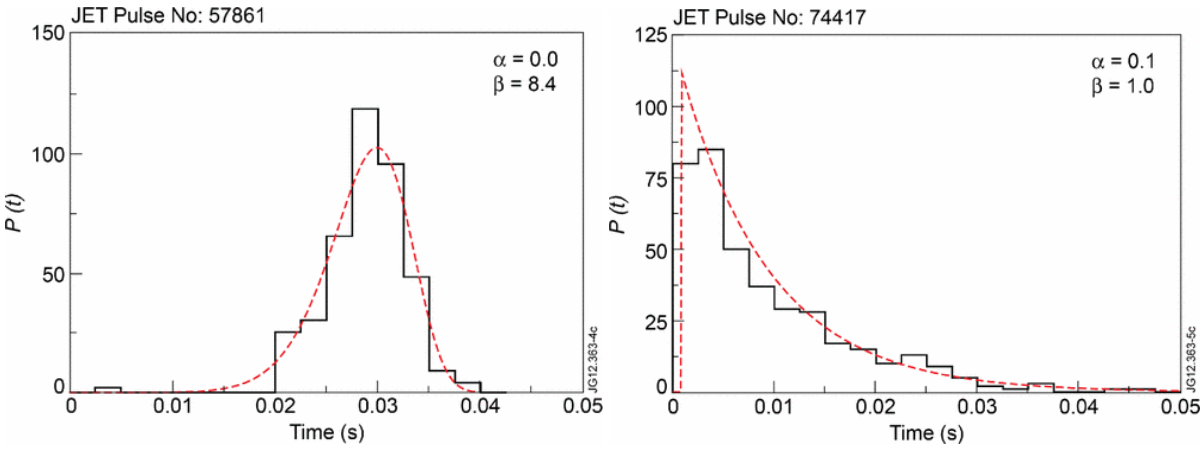

(a) (b)

Weibull (red dashed line) and experimental PDFs (black bar chart), for (a) for JET plasma No. 57861 (type I ELMs) and (b) JET plasma No. 74417 (type III ELMs)

The signature of evolving turbulence in quiet solar wind as seen by Ulysses

Astrophysical Journal 679, 862 (2008) doi:10.1086/586732

Nicol, RM; Chapman, SC; Dendy, RO

Solar wind fluctuations, such as magnetic field or velocity, show power-law power spectra suggestive both of an inertial range of intermittent turbulence (with ~–5/3 exponent), and at lower frequencies, of fluctuations of coronal origin (with ~–1 exponent). The *Ulysses* spacecraft spent many months in the quiet fast solar wind above the Sun's polar coronal holes in a highly ordered magnetic field. We use statistical analysis methods such as the generalized structure function (GSF) and extended self-similarity (ESS) to quantify the scaling of the moments of the probability density function of fluctuations in the magnetic field. The GSFs give power law scaling in the f^{-1} range of the form $\langle |y(t+\tau)-y(t)|^m \rangle \sim \tau^{\zeta(m)}$, but ESS is required to reveal scaling in the inertial range, which is of the form $\langle |y(t+\tau)-y(t)|^m \rangle \sim [g(\tau)]^{\zeta(m)}$. We find that $g(\tau)$ is independent of spacecraft position and $g(\tau) \sim \tau^{-\log_{10}(\bar{\lambda}\tau)}$. The f^{-1} scaling fluctuates with radial spacecraft position. This confirms that, whereas the f^{-1} fluctuations are directly influenced by the corona, the inertial range fluctuations are consistent with locally evolving turbulence, but with an envelope $g(\tau)$, which captures the formation of the quiet fast solar wind.

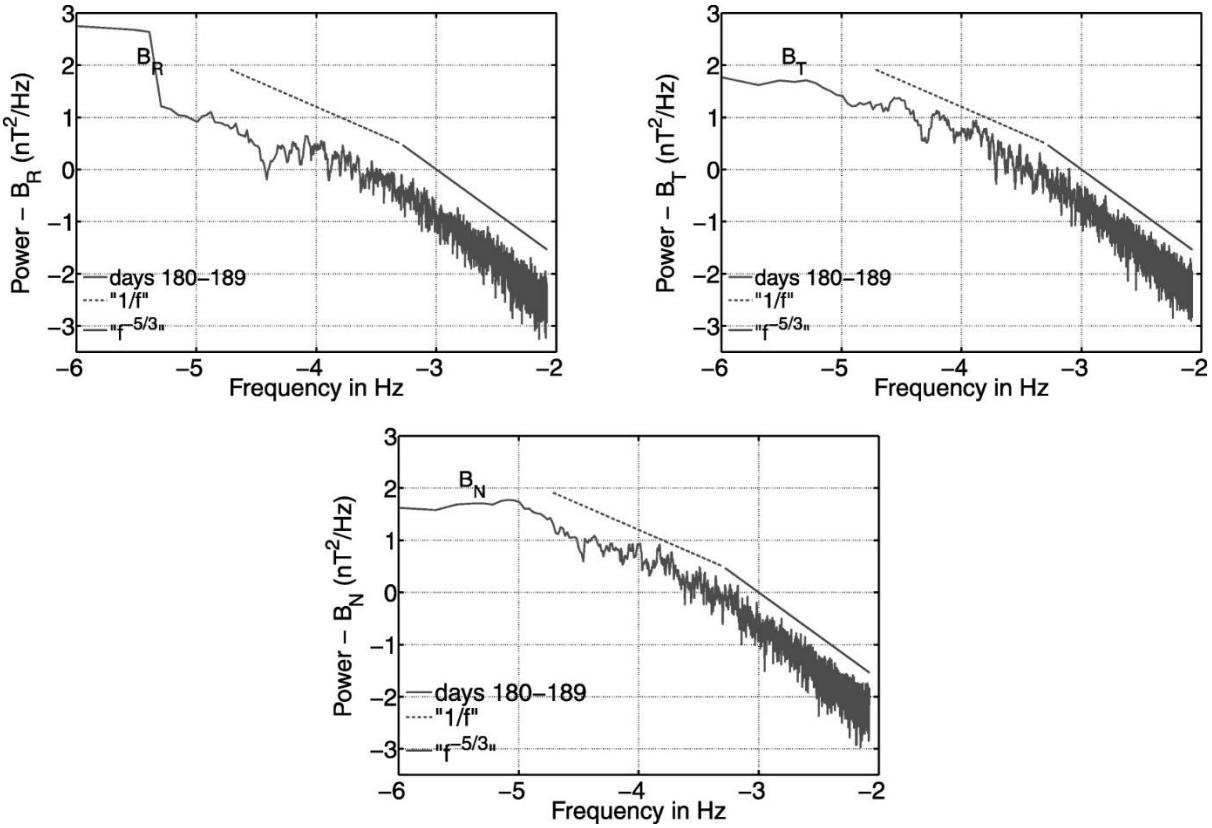

Log-log plots of the *B*-field components' power spectra for days 180-189. Two regions with different scaling exponents are distinguishable, with a break between frequencies at $10^{-3.5}$-10^{-3} Hz, consistent with previous results (Horbury et al. 1996a). For comparison purposes, the –1 and –5/3 power scaling laws are also shown. The power spectra for the other time intervals examined show similar behavior

Statistical properties of edge plasma turbulence in the Large Helical Device

Plasma Physics and Controlled Fusion 50, 095013 (2008) doi:10.1088/0741-3335/50/9/095013

Dewhurst, J.M., Hnat, B., Ohno, N., Dendy, R.O., Masuzaki, S., Morisaki, T., Komori, A

Ion saturation current (I_{sat}) measurements made by three tips of a Langmuir probe array in the Large Helical Device are analysed for two plasma discharges. Absolute moment analysis is used to quantify properties on different temporal scales of the measured signals, which are bursty and intermittent. Strong coherent modes in some datasets are found to distort this analysis and are consequently removed from the time series by applying bandstop filters. Absolute moment analysis of the filtered data reveals two regions of power-law scaling, with the temporal scale $\tau \approx 40$ μs separating the two regimes. A comparison is made with similar results from the Mega-Amp Spherical Tokamak. The probability density function is studied and a monotonic relationship between connection length and skewness is found. Conditional averaging is used to characterize the average temporal shape of the largest intermittent bursts.

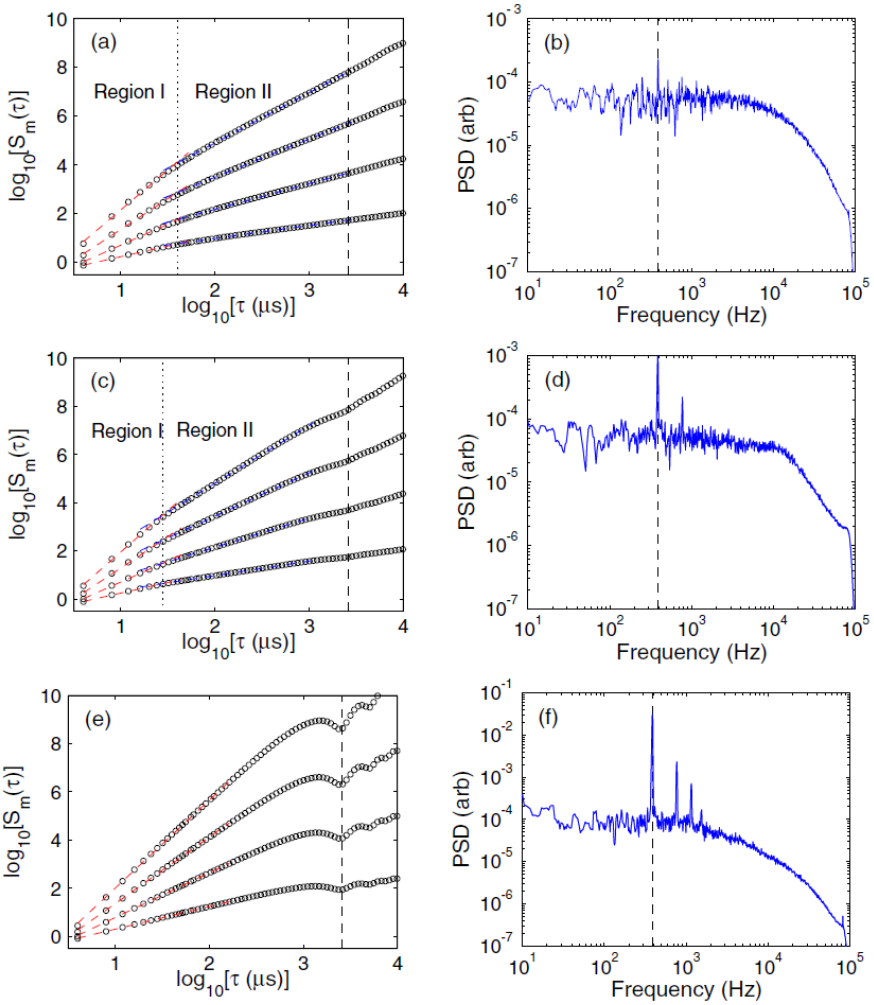

Absolute moments of order 1< m < 4 (left) and PSD (right) for LHD plasma 44190:
(a) and (b) tip 16(s); (c) and (d) tip 17(l); (e) and (f) tip 18(m).
The dashed line on each plot of absolute moments corresponds to the reciprocal of the frequency of the coherent mode marked on the PSD.

Modelling the measured local time evolution of strongly nonlinear heat pulses in the Large Helical Device.

Plasma Physics and Controlled Fusion, 55, (2013) doi:10.1088/0741-3335/55/11/115009

R O Dendy, S C Chapman and S Inagaki

In some magnetically confined plasmas, an applied pulse of rapid edge cooling can trigger either a positive or negative excursion in the core electron temperature from its steady state value. We present a new model which captures the time evolution of the transient, non-diffusive local dynamics in the core plasma. We show quantitative agreement between this model and recent spatially localized measurements (Inagaki et al 2010 Plasma Phys. Control. Fusion 52 075002) of the local time-evolving temperature pulse in cold pulse propagation experiments in the Large Helical Device.

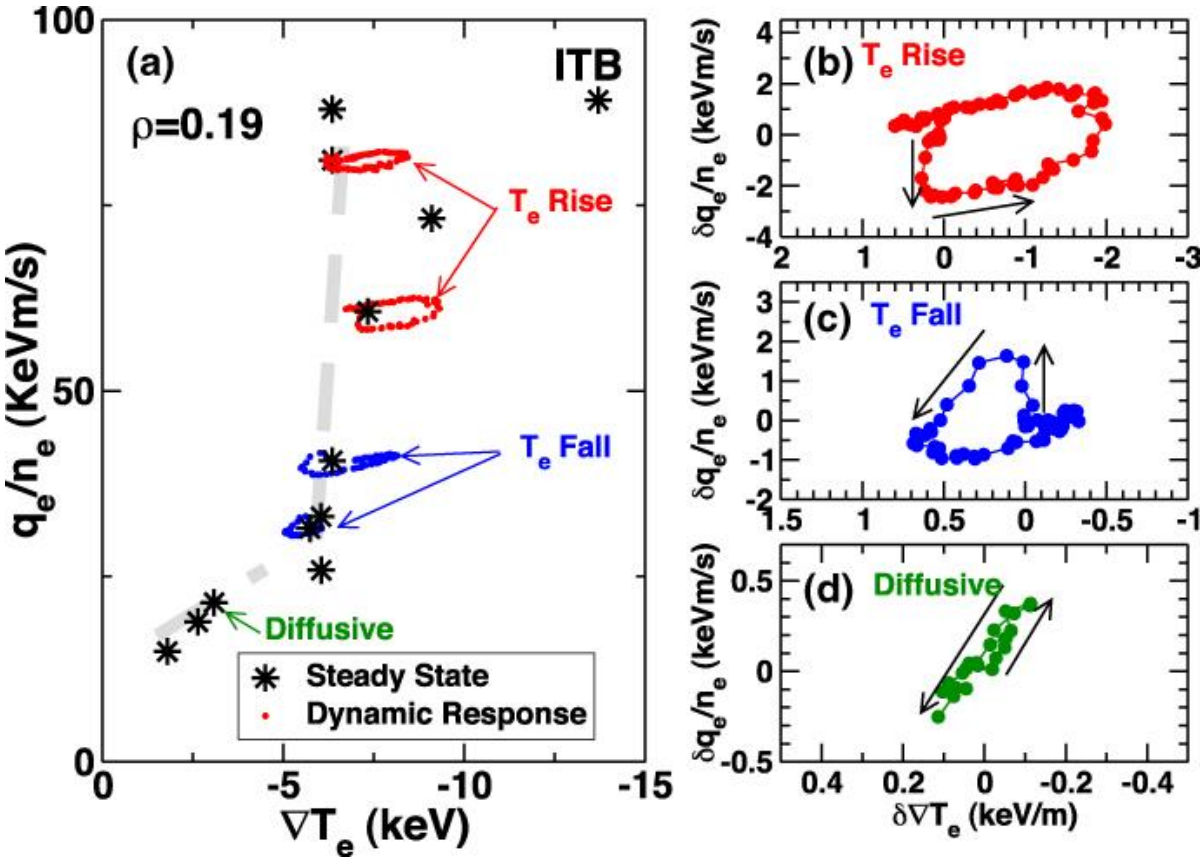

Response of the core plasma to rapid edge cooling as seen in LHD [19]. (*a*) plots the core plasma conditions in the experiments at steady state. The three distinct transient responses to rapid edge cooling are shown in (*b*)–(*d*) and are a sharp temperature rise, a sharp temperature drop, and diffusive transport respectively. The corresponding core plasma conditions for each of these responses are indicated in (*a*).

Self-consistent nonlinear kinetic simulations of the anomalous Doppler instability of suprathermal electrons in plasmas.

Physics of Plasmas, 20, 102122 (2013) http://dx.doi.org/10.1063/1.4827207

W. N. Lai, S. C. Chapman and R. O. Dendy

Suprathermal tails in the distributions of electron velocities parallel to the magnetic field are found in many areas of plasma physics, from magnetic confinement fusion to solar system plasmas. Parallel electron kinetic energy can be transferred into plasma waves and perpendicular gyration energy of particles through the anomalous Doppler instability (ADI), provided that energetic electrons with parallel velocities vjj ðx þ XceÞ=kjj are present; here Xce denotes electron cyclotron frequency, x the wave angular frequency, and kjj the component of wavenumber parallel to the magnetic field. This phenomenon is widely observed in tokamak plasmas. Here, we present the first fully self-consistent relativistic particle-in-cell simulations of the ADI, spanning the linear and nonlinear regimes of the ADI. We test the robustness of the analytical theory in the linear regime and follow the ADI through to the steady state. By directly evaluating the parallel and perpendicular dynamical contributions to j E in the simulations, we follow the energy transfer between the excited waves and the bulk and tail electron populations for the first time. We find that the ratio Xce=ðxpe þ XceÞ of energy transfer between parallel and perpendicular, obtained from linear analysis, does not apply when damping is fully included, when we find it to be xpe=ðxpe þ XceÞ; here xpe denotes the electron plasma frequency. We also find that the ADI can arise beyond the previously expected range of plasma parameters, in particular when Xce > xpe. The simulations also exhibit a spectral feature which may correspond to the observations of suprathermal narrowband emission at xpe detected from low density tokamak plasmas.

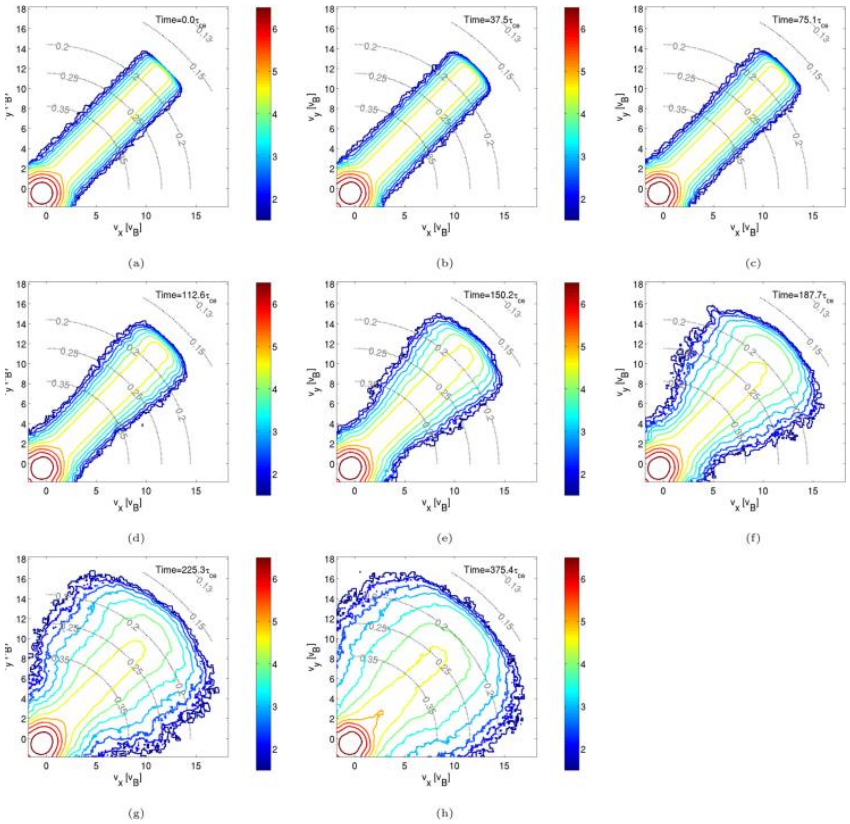

Kinetic Signatures and Intermittent Turbulence in the Solar Wind Plasma

Phys Rev. Lett. 108, 261103 (2012) DOI: http://dx.doi.org/10.1103/PhysRevLett.108.261103

K. T. Osman, W. H. Matthaeus, B. Hnat, and S. C. Chapman

A connection between kinetic processes and intermittent turbulence is observed in the solar wind plasma using measurements from the Wind spacecraft at 1 A.U. In particular, kinetic effects such as temperature anisotropy and plasma heating are concentrated near coherent structures, such as current sheets, which are nonuniformly distributed in space. Furthermore, these coherent structures are preferentially found in plasma unstable to the mirror and firehose instabilities. The inhomogeneous heating in these regions, which is present in both the magnetic field parallel and perpendicular temperature components, results in protons at least 3–4 times hotter than under typical stable plasma conditions. These results offer a new understanding of kinetic processes in a turbulent regime, where linear Vlasov theory is not sufficient to explain the inhomogeneous plasma dynamics operating near non-Gaussian structures.

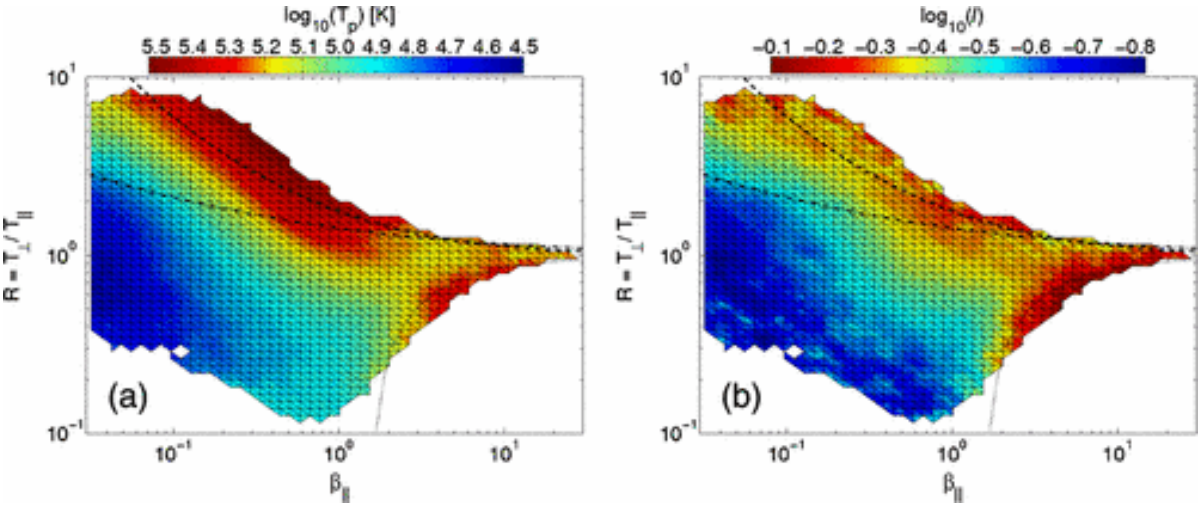

Plot of median (a) scalar proton temperature T_p, and (b) PVI statistic I over the ($\beta_{\parallel}$, $T_{\perp}/T_{\parallel}$) plane. The curves indicate theoretical growth rates for the mirror (dashed line), cyclotron (dot-dashed line), and oblique firehose (dotted line) instabilities. There is a manifest association between these thresholds, hot plasma, and enhanced PVI.

Non-axisymmetric anisotropy of solar wind turbulence

Phys. Rev. Lett., 107,095002, (2011) DOI: http://dx.doi.org/10.1103/PhysRevLett.107.095002

A. J. Turner, G. Gogoberidze, S. C. Chapman, B. Hnat, W. -C. Mueller

A key prediction of turbulence theories is frame-invariance, and in magnetohydrodynamic (MHD) turbulence, axisymmetry of fluctuations with respect to the background magnetic field. Paradoxically the power in fluctuations in the turbulent solar wind are observed to be ordered with respect to the bulk macroscopic flow as well as the background magnetic field. Here, nonaxisymmetry across the inertial and dissipation ranges is quantified using *in situ* observations from Cluster. The observed inertial range nonaxisymmetry is reproduced by a "fly through" sampling of a direct numerical simulation of MHD turbulence. Furthermore, fly through sampling of a linear superposition of transverse waves with axisymmetric fluctuations generates the trend in nonaxisymmetry with power spectral exponent. The observed nonaxisymmetric anisotropy may thus simply arise as a sampling effect related to Taylor's hypothesis and is not related to the plasma dynamics itself.

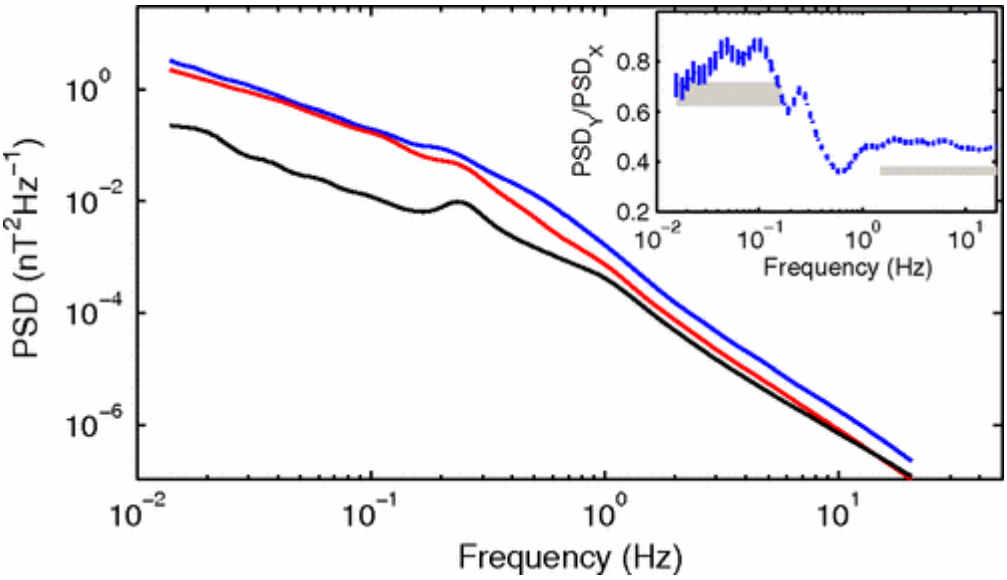

Power Spectral Density (PSD) of magnetic field components (from bottom to top) PSD_z (black), PSD_y (red), and PSD_x (blue), where $\mathbf{e}_z=\mathbf{B}/|\mathbf{B}|$, $\mathbf{e}_x=\mathbf{e}_z\times\mathbf{V}/|\mathbf{e}_z\times\mathbf{V}|$ and $\mathbf{e}_y=\mathbf{e}_z\times\mathbf{e}_x$. Error bars are always smaller than 4% and are usually smaller than the linewidth. The inset shows the ratio of perpendicular PSDs PSD_y/PSD_x.

Finite Larmor radius effects on test particle transport in drift wave-zonal flow turbulence

Plasma Phys. Control. Fusion 52, 025004 (2010) doi:10.1088/0741-3335/52/2/025004

Dewhurst, JM; Hnat, B; Dendy R. O.

The effect of finite Larmor radius on the transport of passive charged test particles moving in turbulent electrostatic fields is investigated. The turbulent field is governed by a flexible model which is able to produce turbulence where zonal flows are damped or free to self-generate. A subtle interplay between trapping in small scale vortices and entrainment in larger scale zonal flows determines the rate, character and Larmor radius dependence of the test particle transport. When zonal flows are damped, the transport is classically diffusive, with Gaussian statistics, and the rate of transport decreases with increasing Larmor radius. Once the Larmor radius is larger than the typical radius of the turbulent vortices, the rate of transport remains roughly constant. When zonal flows are allowed non-Gaussian statistics are observed. Radial transport (across the zones) is subdiffusive and decreases with the Larmor radius at a slower rate. Poloidal transport (along the zones), however, is superdiffusive and increases with small values of the Larmor radius.

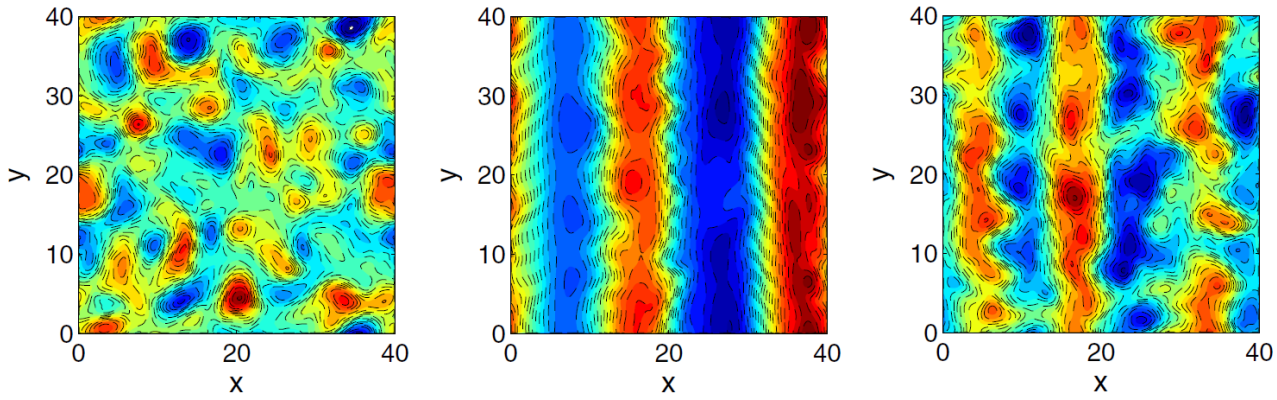

Snapshot of potential ϕ in the saturated quasi-stationary turbulent state for three related models: (left) HW defined by equations (1) and (2) where zonal flows are damped; (centre) MHW defined by equations (5) and (6) allowing the self-generation of zonal flows; (right) intermediate state of MHW where total kinetic energy of zonal flows is set equal to that of non-zonal drift wave turbulence at each time step.

Proton Kinetic Effects and Turbulent Energy Cascade Rate in the Solar Wind

Phys. Rev. Lett., 111, 201101 (2013) DOI: http://dx.doi.org/10.1103/PhysRevLett.111.201101

K.T. Osman, W.H. Matthaeus, K.H. Kiyani, B. Hnat, and S.C. Chapman

The first observed connection between kinetic instabilities driven by proton temperature anisotropy and estimated energy cascade rates in the turbulent solar wind is reported using measurements from the Wind spacecraft at 1 AU. We find enhanced cascade rates are concentrated along the boundaries of the ($\beta_{\parallel}$, $T_{\perp}/T_{\parallel}$) plane, which includes regions theoretically unstable to the mirror and firehose instabilities. A strong correlation is observed between the estimated cascade rate and kinetic effects such as temperature anisotropy and plasma heating, resulting in protons 5–6 times hotter and 70%–90% more anisotropic than under typical isotropic plasma conditions. These results offer new insights into kinetic processes in a turbulent regime.

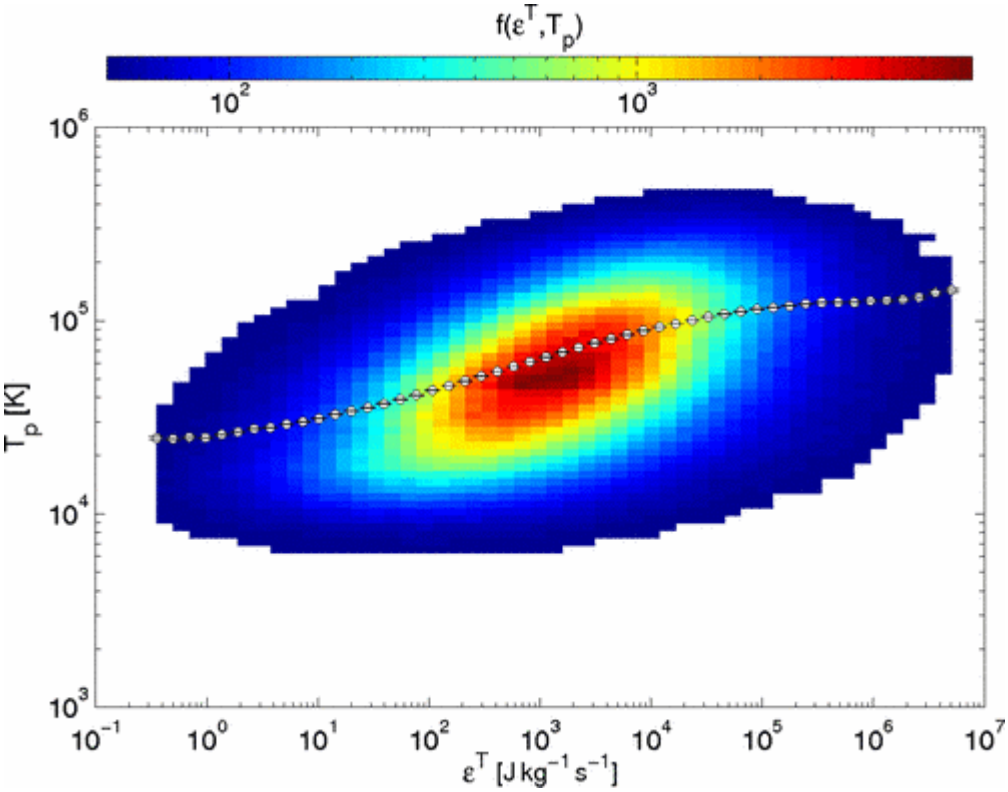

Joint histogram between total turbulence cascade rate and proton temperature, where the mean T_p in each cascade rate bin is represented by a white dot. There is a clear correlation between enhanced T_p and high energy cascade rates.

System Size Effects on Gyrokinetic Turbulence

Physical Review Letters 105, 155001 (2010) http://dx.doi.org/10.1103/PhysRevLett.105.155001

McMillan, BF; Lapillonne, X; Brunner, S; Villard, L; Jolliet, S; Bottino, A; Gorler, T; Jenko, F

The scaling of turbulence-driven heat transport with system size in magnetically confined plasmas is reexamined using first-principles based numerical simulations. Two very different numerical methods are applied to this problem, in order to resolve a long-standing quantitative disagreement, which may have arisen due to inconsistencies in the geometrical approximation. System size effects are further explored by modifying the width of the strong gradient region at fixed system size. The finite width of the strong gradient region in gyroradius units, rather than the finite overall system size, is found to induce the diffusivity reduction seen in global gyrokinetic simulations.

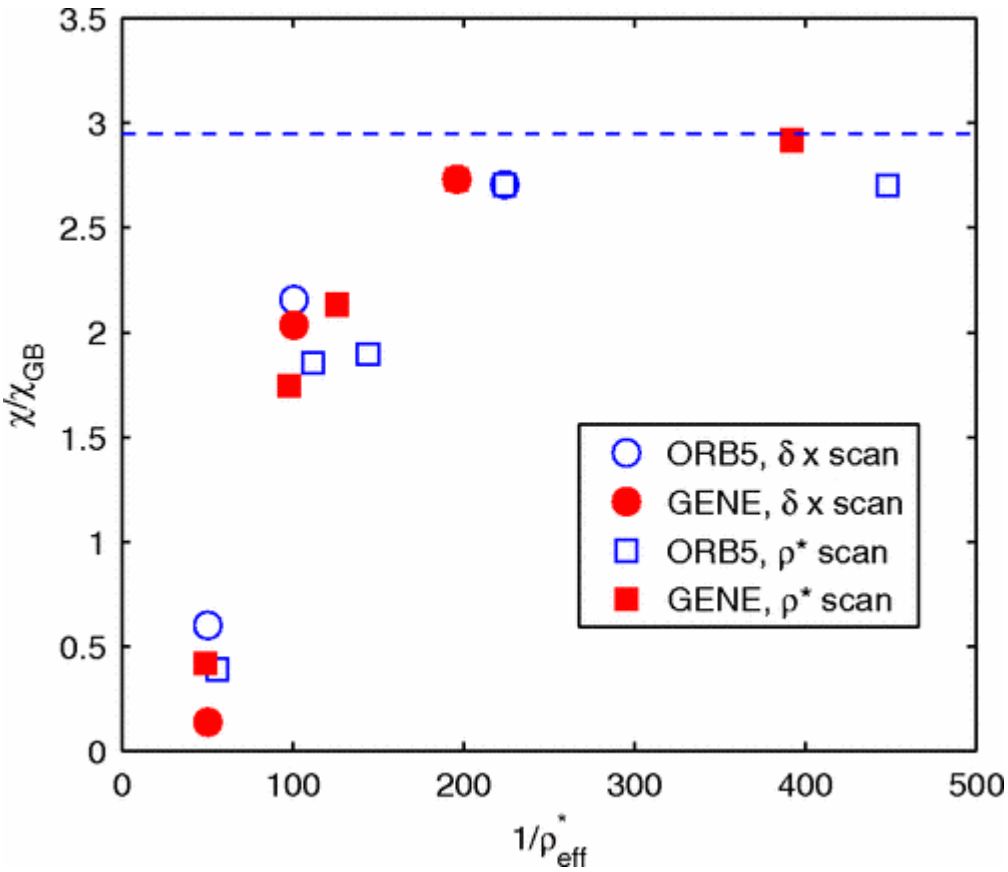

Average flux levels $r \in [0.4,0.6]$ for $t \in [150,410]R/c_s$ versus the width of the strong gradient region, $1/\rho_{\mathrm{eff}}^{*}$, in gyroradius units.

Role of Plasma Elongation on Turbulent Transport in Magnetically Confined Plasmas

Physical Review Letters 102, 195002 (2009) http://dx.doi.org/10.1103/PhysRevLett.102.195002

Angelino, P; Garbet, X; Villard, L; Bottino, A; Jolliet, S; Ghendrih, P; Grandgirard, V; McMillan, B; Y. Sarazin, G. Dif-Pradalier, T. M. Tran

The theoretical study of plasma turbulence is of central importance to fusion research. Experimental evidence indicates that the confinement time results mainly from the turbulent transport of energy, the magnitude of which depends on the turbulent state resulting from nonlinear saturation mechanisms, in particular, the self-generation of coherent macroscopic structures and large scale flows. Plasma geometry has a strong impact on the structure and magnitude of these flows and also modifies the mode linear growth rates. Nonlinear global gyrokinetic simulations in realistic tokamak magnetohydrodynamic equilibria show how plasma shape can control the turbulent transport. Results are best described in terms of an effective temperature gradient. With increasing plasma elongation, the nonlinear critical effective gradient is not modified while the stiffness of transport is decreasing.

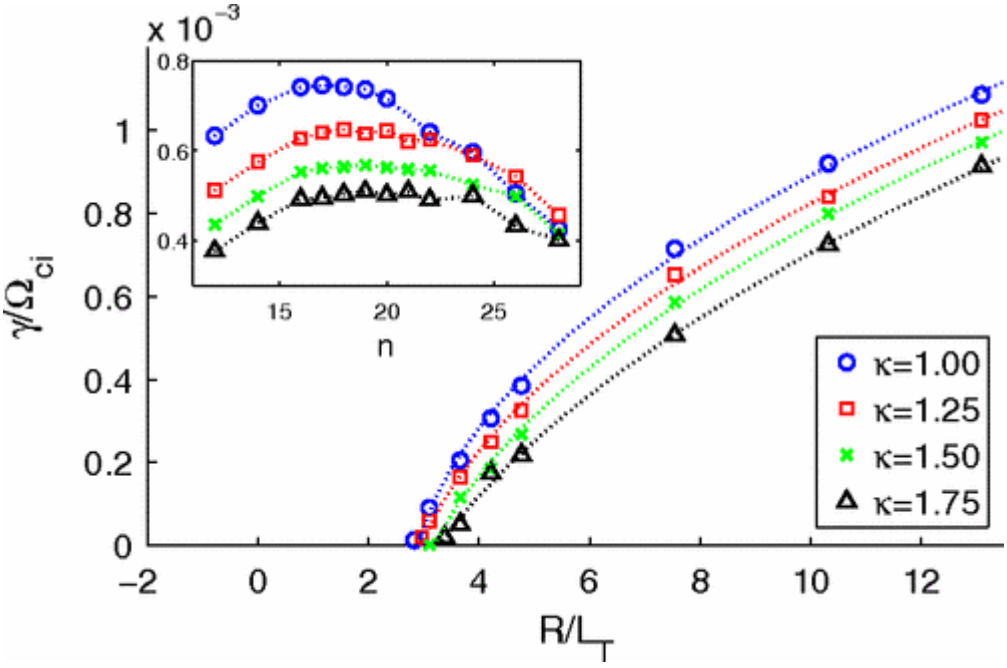

Linear growth rates of the linearly most unstable global ITG mode as a function of the temperature gradient scale length R/L_T and of the edge elongation. The stabilizing effect of the elongation is observable for all values of the temperature gradient. ITG linear growth rates as a function of the toroidal mode number n are plotted in the top-left corner. Growth rates are normalized to the ion cyclotron frequency Ω_{ci}.

Long global gyrokinetic simulations: Source terms and particle noise control

Physics of Plasmas, 15, 052308 (2008) http://dx.doi.org/10.1063/1.2921792

McMillan, BF; Jolliet, S; Tran, TM; Villard, L; Bottino, A; Angelino, P

In global gyrokinetic simulations it takes a long time for the turbulence to reach a quasisteady state, and quantitative predictions about the quasisteady state turbulence have been difficult to obtain computationally. In particular, global particle-in-cellgyrokinetic simulations have been inefficient for long simulations due to the accumulation of noise. It is demonstrated that a simple Krook operator can effectively control noise; it also introduces an unphysical dissipation, which damps the zonal flows and can significantly affect simulation results even when the relaxation time is very long. However, it is possible to project out the effects of the Krook operator on the zonal flows. This permits noise accumulation to be controlled while preserving the physics of interest; simulations are then run to determine the level of quasisteady state transport and the variation across the ensemble of turbulentdynamics. Convergence is demonstrated both in the number of computational particles and the unphysical relaxation time.

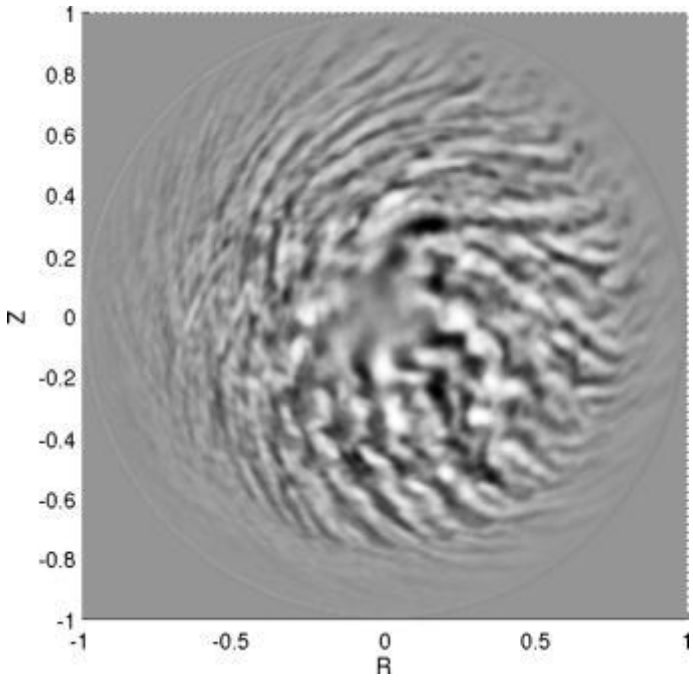

Nonzonal electric potential (as grey levels) on the plasma cross section in the late-time saturated phase of the simulation with $R/L_{T0}=7.2$ (solid lines) and a Krook operator with $\gamma_S=1.26\times10^{-2}(c_s/a)$.

Avalanche like bursts in global gyrokinetic simulations

Physics of Plasmas 16, 022310 (2009) http://dx.doi.org/10.1063/1.3079076

McMillan, B.F., Jolliet, S., Tran, T.M., Villard, L., Bottino, A., Angelino, P.

Highly variable flux surface averaged heat fluxes are resolved in gyrokinetic simulations of ion temperature gradient(ITG)turbulence, even in large systems. Radially propagating fronts or *avalanches* are also seen. Their propagation lengths in gyroradii and relative amplitude remain constant as simulation size is increased, so the avalanches appear to result from local dynamics, rather than global relaxation events. For the Cyclone [Dimits *et al.*, Phys. Plasmas7, 969 (2000)] case, the avalanche propagation direction is found to depend on the sign of the shearing rate. A mechanism for avalanche propagation based on the advection of turbulence tilted by the shear flows is proposed: The Cyclone linear ITG dispersion relation explains the propagation direction of tilted vortices. It also explains why there is no such preferred direction in a simulation with reduced magnetic shear. The paper explores several models for these bursts. First, certain types of models based on nonlinear heat diffusion equations are ruled out. A different type of one-dimensional (1D) model, introduced in Benkadda *et al.* [Nucl. Fusion41, 995 (2001)], yields much better qualitative and quantitative agreement. However, the 1D model cannot explain the directionality of the bursts, even though it includes the features typically considered important for burst propagation. A symmetry-breaking term is necessary. An additional term is included to reproduce the wave dispersion with respect to radial wavenumber, and this is shown to be sufficient to reproduce the favored direction for burst propagation.

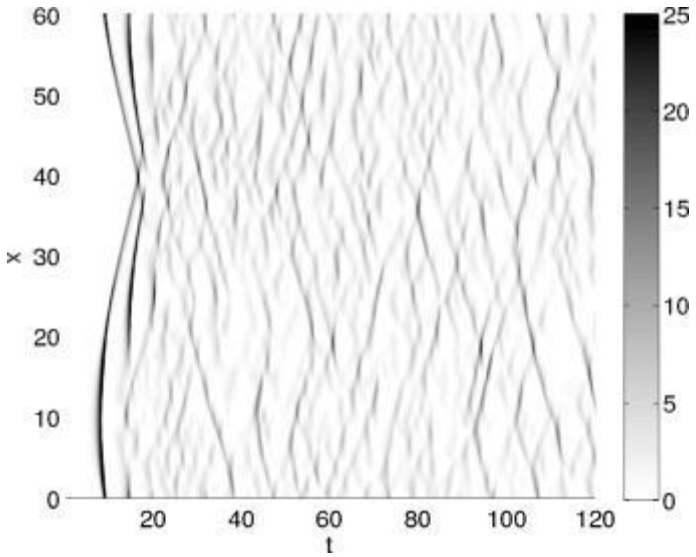

Flux vs time and radius in the 1D model of ITG turbulence with a background shear flow $E'_0=0.15$.

Probing Warm Dense Lithium by Inelastic X-Ray Scattering

Nature Physics 4, 940-944 (2008) doi: 10.1038/nphys1103

E. Garcia Saiz, G. Gregori, D.O. Gericke, J. Vorberger, B. Barbrel, R.J. Clarke, R.R. Freeman, S.H. Glenzer, F.Y. Khattak, M. Koenig, O.L. Landen, D. Neely, P. Neumayer, M.M. Notley, A. Pelka, D. Price, M. Roth, M. Schollmeier, R.L. Weber, L. van Woerkom, K. Wuensch and D. Riley

One of the grand challenges of contemporary physics is understanding strongly interacting quantum systems comprising such diverse examples as ultracold atoms in traps, electrons in high-temperature superconductors and nuclear matter. Warm dense matter, defined by temperatures of a few electron volts and densities comparable with solids, is a complex state of such interacting matter. Moreover, the study of warm dense matter states has practical applications for controlled thermonuclear fusion, where it is encountered during the implosion phase, and it also represents laboratory analogues of astrophysical environments found in the core of planets and the crusts of old stars. Here we demonstrate how warm dense matter states can be diagnosed and structural properties can be obtained by inelastic X-ray scattering measurements on a compressed lithium sample. Combining experiments and *ab initio* simulations enables us to determine its microscopic state and to evaluate more approximate theoretical models for the ionic structure.

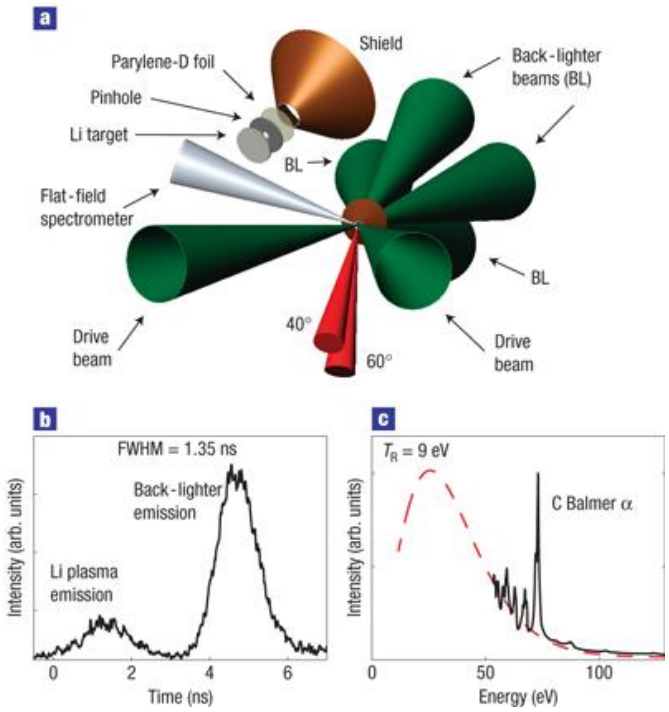

a, Set-up of the experiment, showing the shock-drive and back-lighter beams; the target assembly with a cone shield to avoid undesired signal on the detector, the parylene-D foil, the 170 um collimating pinhole and the Li target; the line of sight of the flat-field spectrometer and the 60˚ and 40˚ positions for the time-integrated Von Hamos spectrometer. The back-lighter beams are all fired inside the cone shield onto the parylene-D foil, while the drive beams are fired onto the Li sample. **b**, Time-resolved X-ray pulse profile at 2.96 keV. The initial signal corresponds to the coronal Li plasma emission from the shock-drive beams. The second peak is associated with the X-ray signal from the parylene-D plasma. **c**, Measured extreme-ultraviolet (space and time integrated) emission spectrum. The background signal is well fitted by a black body with temperature T_R~9±2 eV.

Nonlinear Collisional Absorption of Laser Light

Physical Review Letters 105, 265701 (2010) http://dx.doi.org/10.1103/PhysRevLett.103.065005

A. Grinenko and D.O. Gericke

We present a new theoretical approach for collisional absorption of laser energy in dense plasmas which accommodates arbitrary frequencies and high intensities of the laser field by establishing a connection between laser absorption by inverse bremsstrahlung and the stopping power for ions. This relation is then applied to include strong correlations beyond the mean field approach. The results show excellent agreement with molecular dynamics simulations up to very high coupling strength.

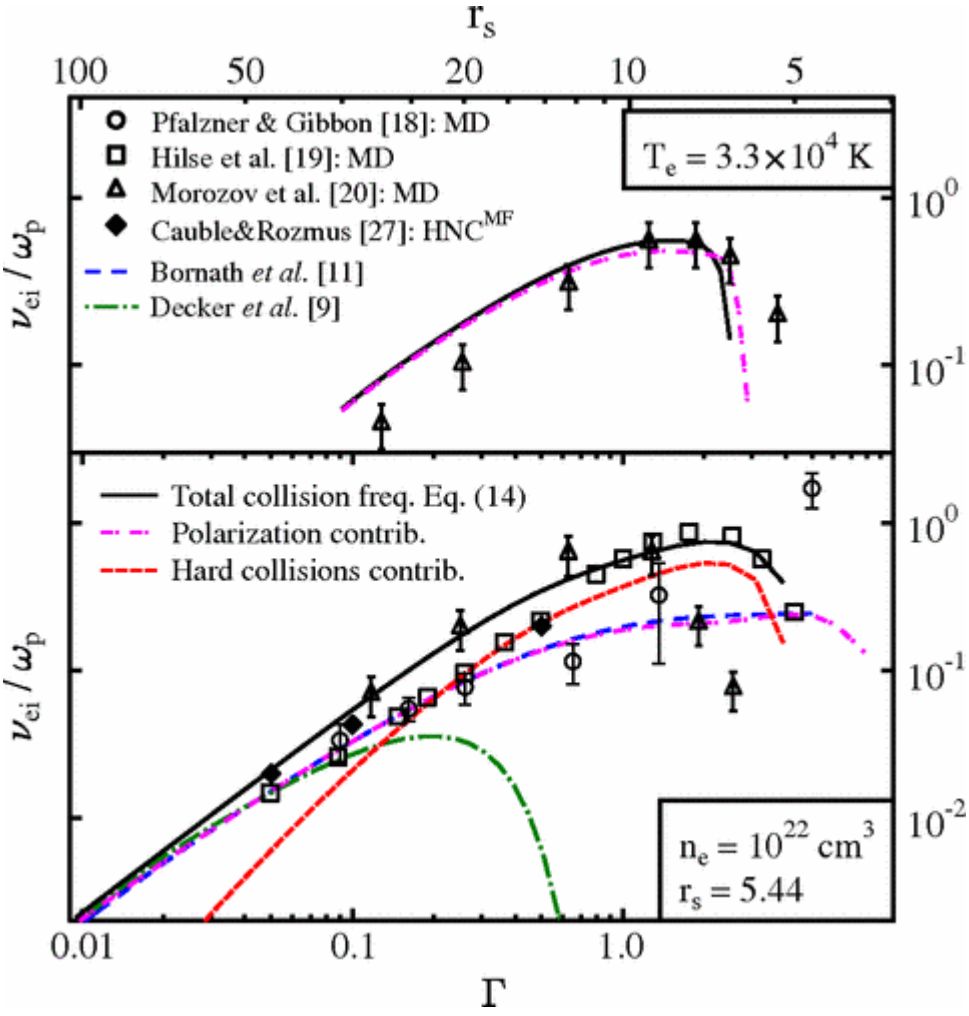

Collision frequency ν_{ei} versus coupling parameter Γ for a hydrogen plasma with fixed temperature and density and a laser field with ω_0/ω_p=1 (upper panel), ω_0/ω_p=3 (lower panel), and v_0/v_{th}=0.2. Solid line: Eq. (14); punctured lines: contributions of hard collisions and polarization to Eq. (14). The classical results of Decker *et al.* [9] were calculated with an integral cutoff at $k_{max}=m_e v_{th}^2/Ze^2$. $r_s=a_e/a_B$, with $a_e=(3/4\pi n_e)^{1/3}$ and a_B being the Bohr radius.

Ultra-fast Melting of Carbon Induced by Intense Proton Beams

Physical Review Letters 105 , 265701 (2010) http://dx.doi.org/10.1103/PhysRevLett.105.265701

A. Pelka, G. Gregori, D.O. Gericke, J. Vorberger, S.H. Glenzer, M. M. Gunther, K. Harres, R. Heathcote, A. Kritcher, N.L. Kugland, B. Li, M. Makita, J. Mithen, D. Neely, C. Niemann, A. Otten, D. Riley, G. Schaumann, M. Schollmeier, An. Tauschwitz and M. Roth

Laser-produced proton beams have been used to achieve ultrafast volumetric heating of carbon samples at solid density. The isochoric melting of carbon was probed by a scattering of x rays from a secondary laser-produced plasma. From the scattering signal, we have deduced the fraction of the material that was melted by the inhomogeneous heating. The results are compared to different theoretical approaches for the equation of state which suggests modifications from standard models.

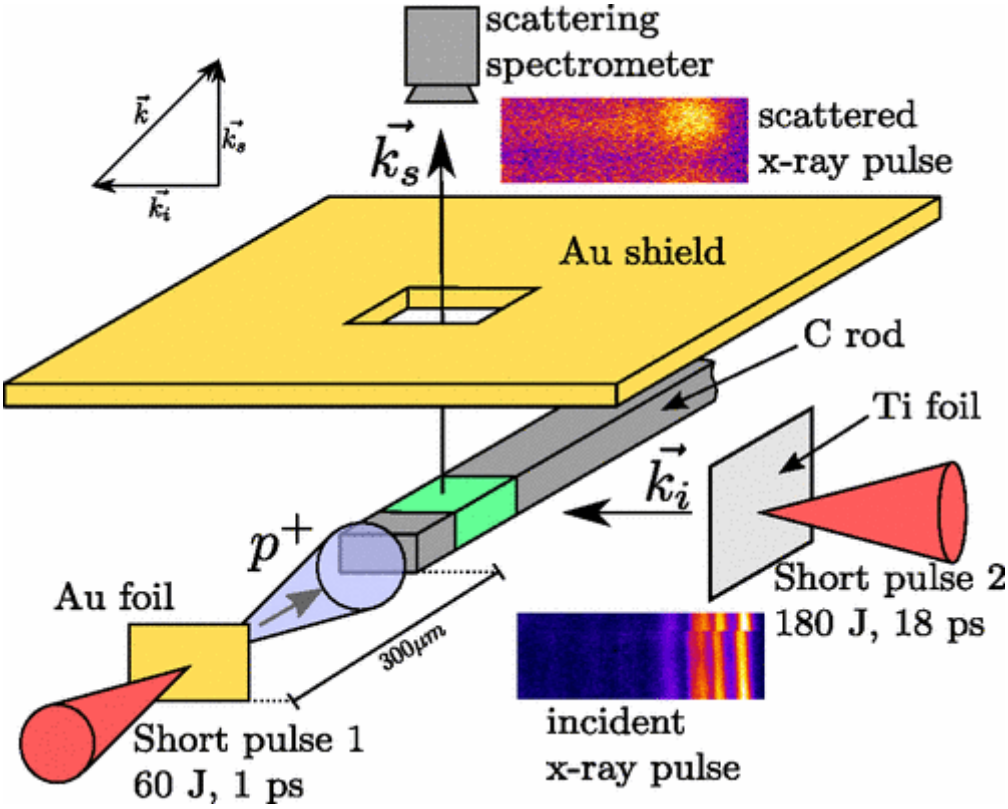

Schematic layout: a polycrystalline graphite rod (125 μm×300 μm×3 mm) is heated by the protons produced by the laser coming from the lower left. The second laser hits a titanium foil to produce an intense x-ray pulse which is scattered off the green region of the sample and detected by a spectrometer above the target at 90°. The gold shielding blocks the line of sight from the laser spots to the scattering spectrometer as well as the front and back regions of the carbon rod. The RCF proton detector and the source radiation spectrometer are not shown.

Analysis of X-Ray Thomson Scattering for Nonequilibrium Plasmas

Physical Review Letters 107, 165004 (2011) http://dx.doi.org/10.1103/PhysRevLett.107.165004

D.A. Chapman and D.O. Gericke

We develop the theory for light scattering as a diagnostic method for plasmas in nonequilibrium states. We show how well-known nonequilibrium features, like beam acoustic modes, arise in the spectra. The analysis of an experiment with strongly driven electrons demonstrates the abilities of the new approach; we find qualitatively different scattering spectra for different times and excellent agreement with the experimental data after time integration. Finally, an analysis of data from dense beryllium suggests that an energetic electron component exists in this experiment as well.

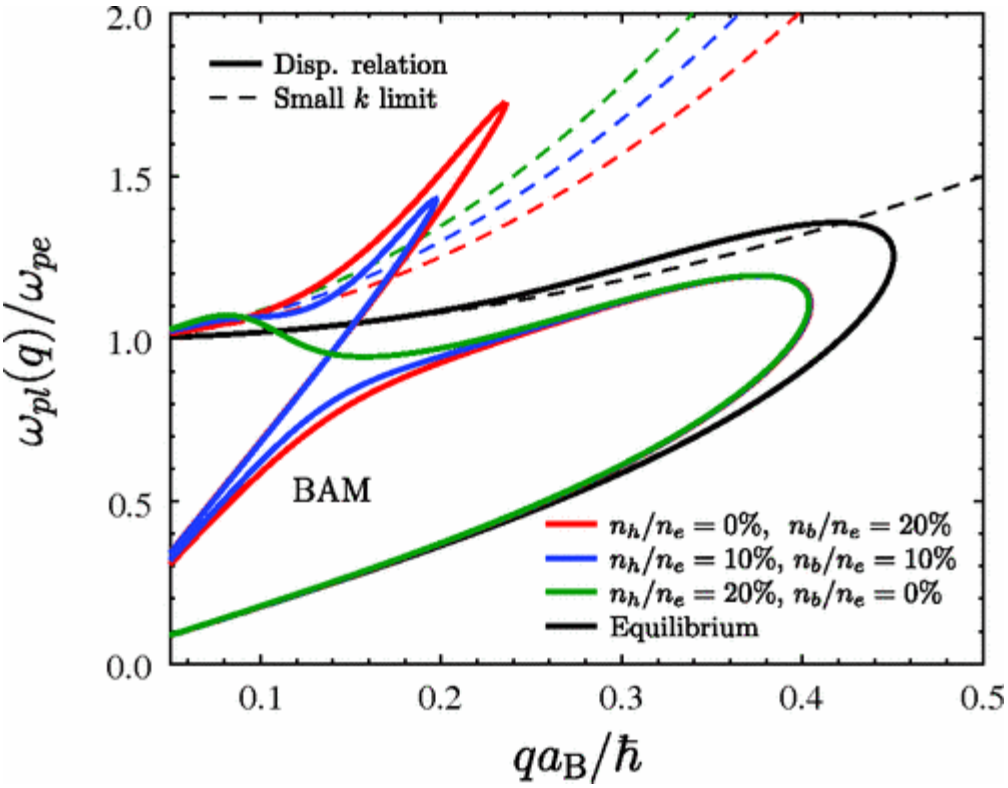

Plasmon dispersion for fully ionized liquid hydrogen (n_e=4.2×10^{22} cm^{-3}) and different ratios of hot and cold electrons (T_c=2 eV, T_h=50 eV, E_b=50 eV). The results of the small q expansion (dashed) are shown for comparison.

Detection of waves in the solar corona: Kink or Alfven?

Astrophysical Journal Letters 676, L73-75, 2008 doi:10.1086/587029

Van Doorsselaere T, Nakariakov VM, Verwichte E

Recently, the omnipresence of waves has been discovered in the corona using the CoMP instrument. We demonstrate that the observational findings can be explained in terms of guided kink magnetoacoustic modes. The interpretation of the observations in terms of Alfvén waves is shown to be inconsistent with MHD wave theory. The implications of the interpretation in terms of kink waves are discussed.

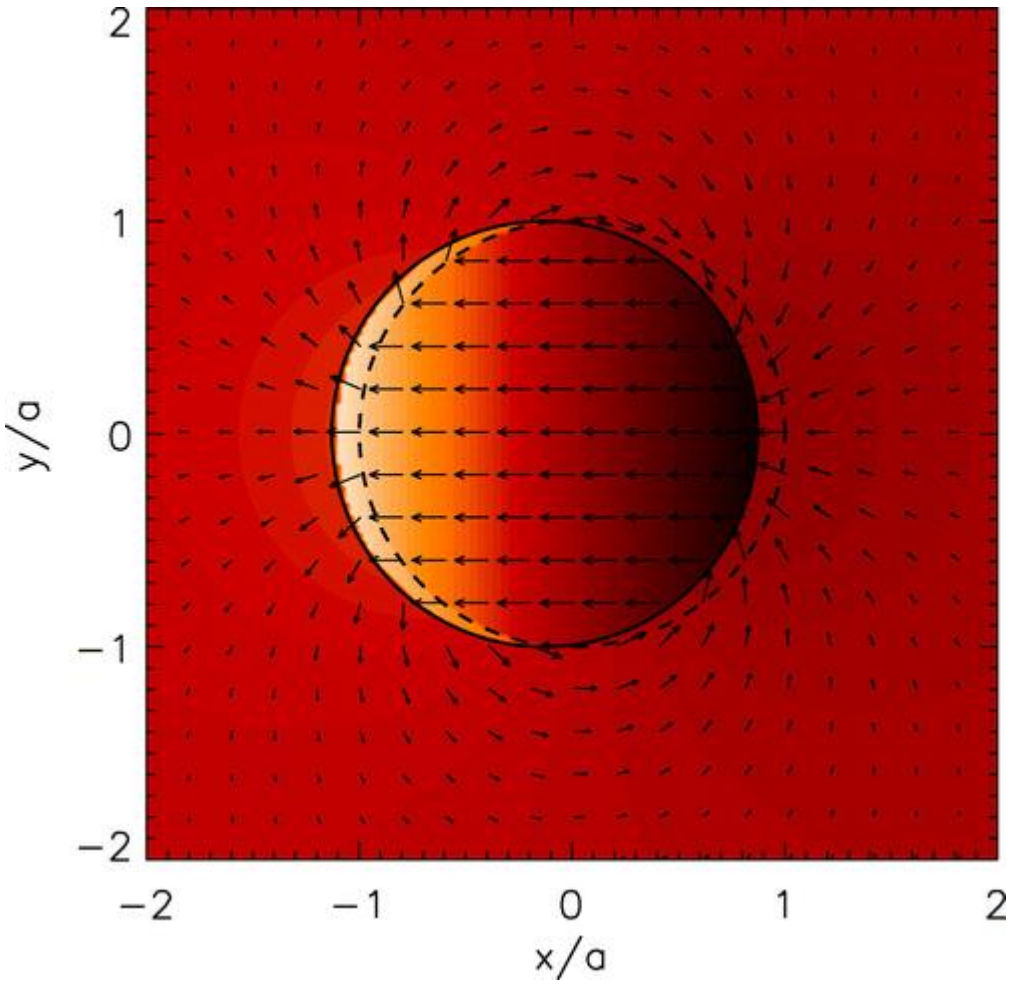

Transverse cut through the cylinder for a fast kink mode. The arrows indicate the velocity profile, and the color shade shows the relative density perturbation (ρ^1/ρ): light colors show a high density perturbation, dark shows the low values.

Quasi-periodic pulsations in the gamma-ray emission of a solar flare

Astrophysical Journal Letters 708, L47-L51, 2010

Nakariakov VM, Foullon C, Myagkova IN, Inglis, AR

Quasi-periodic pulsations (QPP) of gamma-ray emission with a period of about 40 s are found in a single loop X-class solar flare on 2005 January 01 at photon energies up to 2-6 MeV with the SOlar Neutrons and Gamma-rays (SONG) experiment aboard the CORONAS-F mission. The oscillations are also found to be present in the microwave emission detected with the Nobeyama Radioheliograph, and in the hard X-ray and low energy gamma-ray channels of RHESSI. Periodogram and correlation analysis show that the 40 s QPP of microwave, hard X-ray and gamma-ray emission are almost synchronous in all observation bands. Analysis of the spatial structure of hard X-ray and low energy (80-225 keV) gamma-ray QPP with RHESSI reveal synchronous while asymmetric QPP at both footpoints of the flaring loop. The difference between the averaged hard X-ray fluxes coming from the two footpoint sources is found to oscillate with a period of about 13 s for five cycles in the highest emission stage of the flare. The proposed mechanism generating the 40 s QPP is a triggering of magnetic reconnection by a kink oscillation in a nearby loop. The 13 s periodicity could be produced by the second harmonics of the sausage mode of the flaring loop.

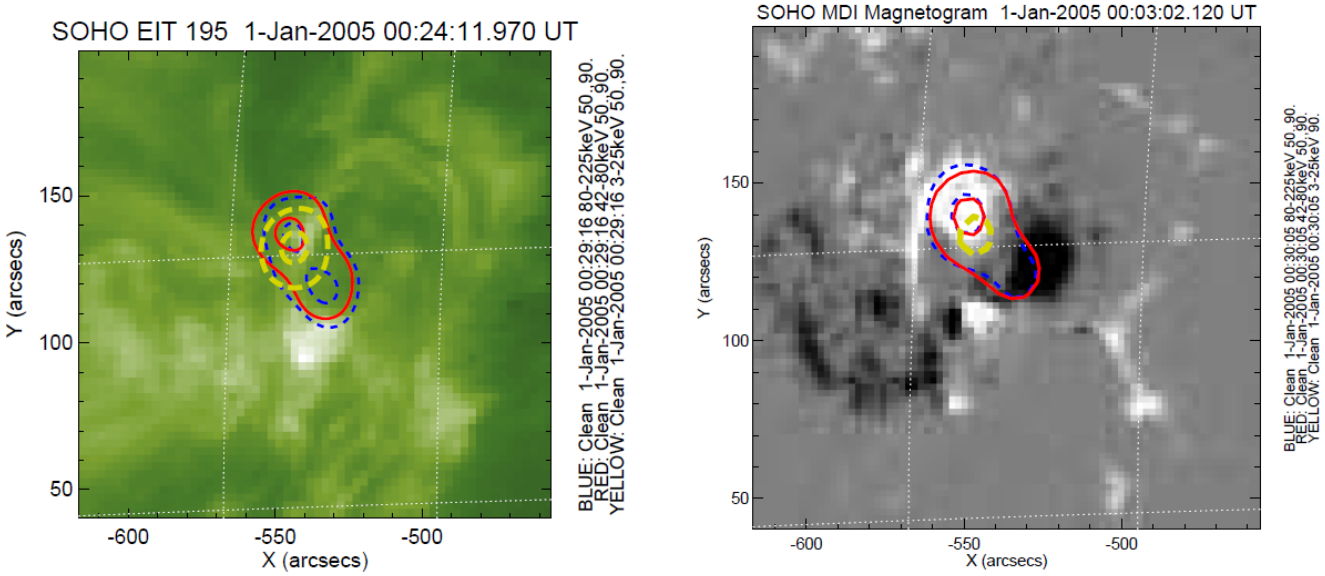

EIT 195 °A image (left panel) and longitudinal magnetic field observed by MDI (right panel) before the QPP in the 2005 January 1 flare. Superimposed are the contour levels at 50 and 90% of the maximum value of RHESSI images (reconstructed from collimators 4F- 7F) (a) between 00:29:16-00:29:20 UT and (b) between 00:30:05-00:30:09 UT. Three energy ranges are shown: 3-25 keV in (yellow) thick long-dashed lines, 42-80 keV in (red) thin solid lines, and 80-225 keV in (blue) thin dashed lines.

Coronal magnetic field measurement using loop oscillations observed by Hinode/EIS

Astronomy & Astrophysics 487, L17-L20, 2008 http://dx.doi.org/10.1051/0004-6361:200810186

Van Doorsselaere T, Nakariakov VM, Young PR, Verwichte, E

We report the first spectroscopic detection of a kink MHD oscillation of a solar coronal structure by the Extreme-Ultraviolet Imaging Spectrometer (EIS) on the Japanese Hinode satellite. The detected oscillation has an amplitude of 1 kms−1 in the Doppler shift of the FeXII 195 Å spectral line (1.3 MK), and a period of 296 s. The unique combination of EIS's spectroscopic and imaging abilities enables us to measure simultaneously the mass density and length of the oscillating loop. This enables us to measure directly the magnitude of the local magnetic field, the fundamental coronal plasma parameter, as 39 ± 8 G, with unprecedented accuracy. This proof of concept makes EIS an exclusive instrument for the full scale implementation of the MHD coronal seismological technique.

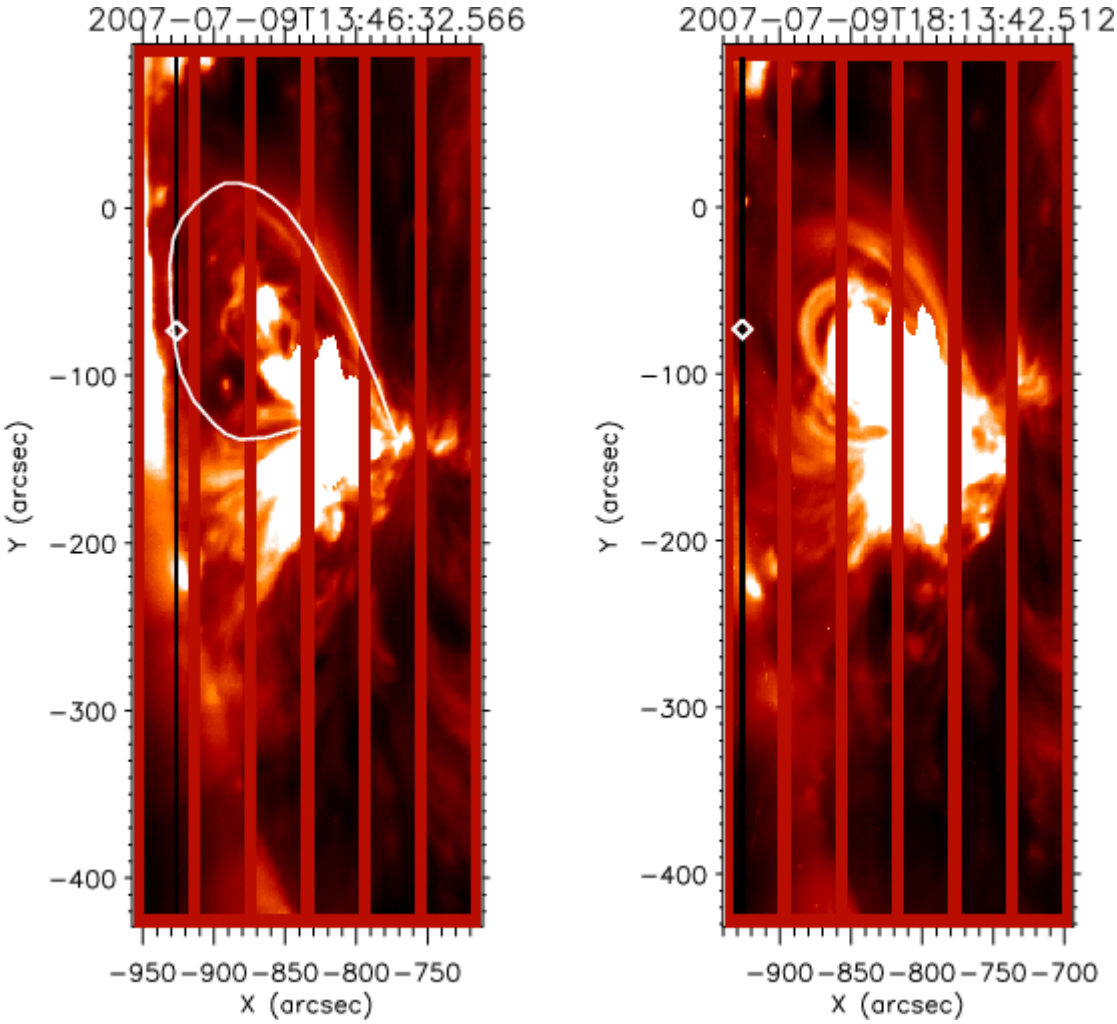

Overview of the observed active region on 2007 July 9 at 13:46 UT (just after the oscillation) and 18:13 UT, respectively, acquired by Hinode/EIS. The colour code is the intensity in the 195 Å line. The vertical black line indicates the position of the slit. The white diamond indicates the pixel showing oscillations. The white line traces out the oscillating loop.

Relationship between wave processes in sunspots and quasi-periodic pulsations in active region flares

Astronomy & Astrophysics 505, 791-799, 2009 http://dx.doi.org/10.1051/0004-6361/200912132

Sych, R; Nakariakov, VM; Karlicky, M; Anfinogentov, S

A phenomenological relationship between oscillations in a sunspot and quasi-periodic pulsations (QPP) in flaring energy releases at an active region (AR) above the sunspot is established. The analysis of the microwave emission recorded by the Nobeyama Radioheliograph at 17 GHz shows a gradual increase in the power of the 3-min oscillation train in the sunspot associated with AR 10756 before flares in this AR. The flaring light curves are found to be bursty with a period of 3 min. Our analysis of the spatial distribution of the 3-min oscillation power implies that the oscillations follow from sunspots along coronal loops towards the flaring site. It is proposed that QPP in the flaring energy releases can be triggered by 3-min slow magnetoacoustic waves leaking from sunspots.

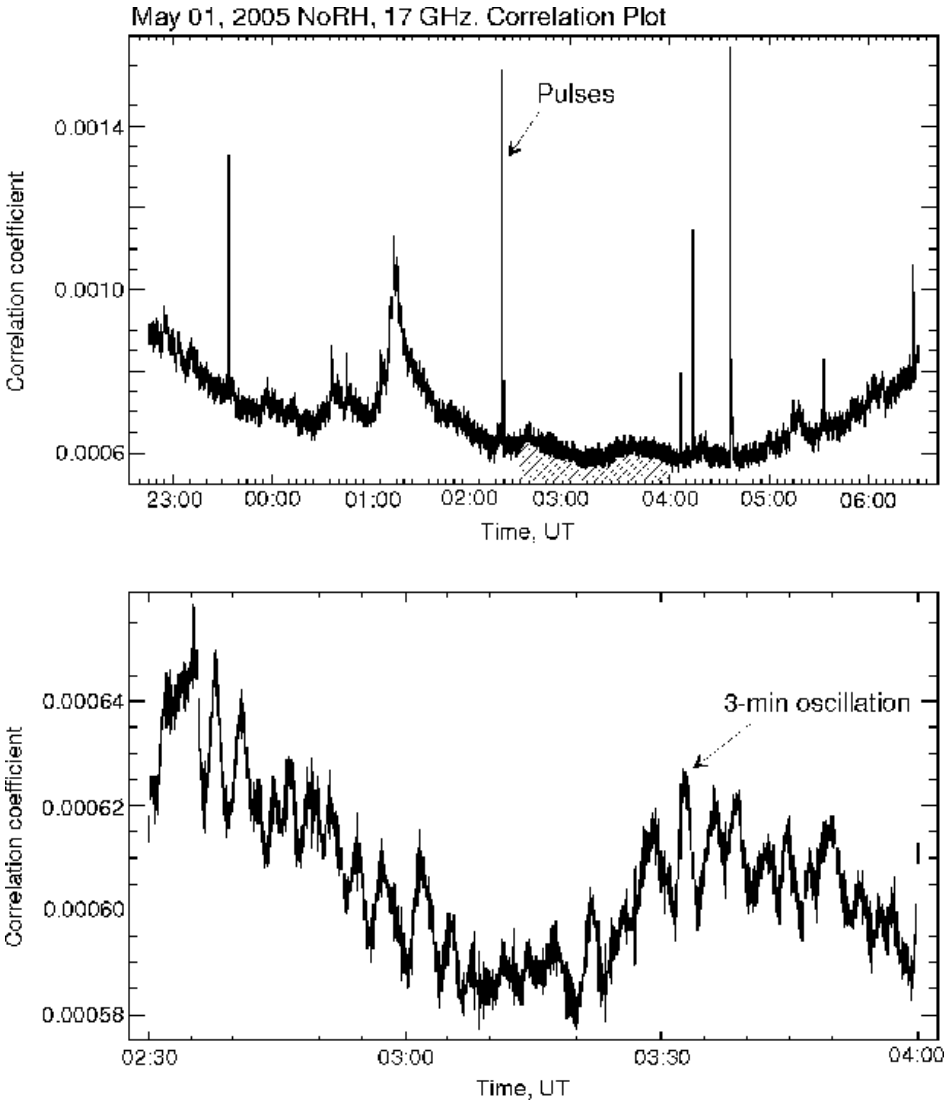

An example of the flaring activity on 2005 May 1: the correlation time profile of NoRH at 17 GHz. The *bottom panel* zooms the time interval hatched in the *upper panel*.

Seismology of a large solar coronal loop from EUVI/STEREO observations of its transverse oscillation

Astrophysical Journal 698 (1), 397-404 (2009) http://dx.doi.org/10.1088/0004-637X/698/1/397

Verwichte, E., Aschwanden, M.J., Van Doorsselaere T., Foullon, C. & Nakariakov, V.M

The first analysis of a transverse loop oscillation observed by both *Solar TErrestrial RElations Observatories* (*STEREO*) spacecraft is presented, for an event on the 2007 June 27 as seen by the Extreme Ultraviolet Imager (EUVI). The three-dimensional loop geometry is determined using a three-dimensional reconstruction with a semicircular loop model, which allows for an accurate measurement of the loop length. The plane of wave polarization is found from comparison with a simulated loop model and shows that the oscillation is a fundamental horizontally polarized fast magnetoacoustic kink mode. The oscillation is characterized using an automated method and the results from both spacecraft are found to match closely. The oscillation period is 630 ± 30 s and the damping time is 1000 ± 300 s. Also, clear intensity variations associated with the transverse loop oscillations are reported for the first time. They are shown to be caused by the effect of line-of-sight integration. The Alfvén speed and coronal magnetic field derived using coronal seismology are discussed. This study shows that EUVI/*STEREO* observations achieve an adequate accuracy for studying long-period, large-amplitude transverse loop oscillations.

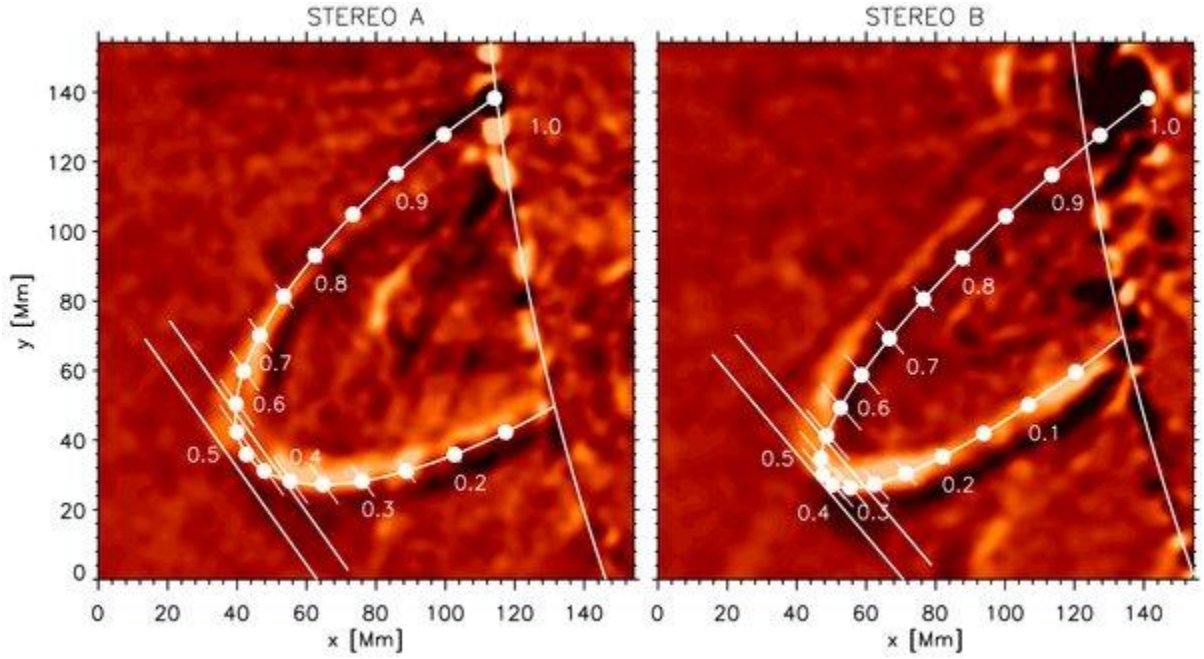

Simulated loop is shown superimposed on a difference image from each *STEREO* spacecraft. The dots mark out the distance along the loop in steps of 0.05 times the loop length. The lines through the dots show the projected direction of the fundamental horizontally polarized kink mode. The two parallel lines outline path used in the oscillation analysis, which is centered on the loop top and parallel to the projected direction of oscillation polarization.

Spatial Seismology of a large Coronal Loop Arcade from TRACE and EIT Observations of its Transverse Oscillations

Astrophysical Journal. 717 (1), 458 (2010) doi:10.1088/0004-637X/717/1/458

Verwichte E., Foullon, C. & Van Doorsselaere, T.

We present a study of transverse loop oscillations in a large coronal loop arcade, using observations from the *Transition Region And Coronal Explorer* (*TRACE*) and Extreme-ultraviolet Imaging Telescope (EIT). For the first time we reveal the presence of long-period transverse oscillations with periods between 24 minutes and 3 hr. One loop bundle, 690 Mm long and with an oscillation period of 40 minutes, is analyzed in detail and its oscillation characteristics are determined in an automated manner. The oscillation quality factor is similar to what has been found earlier for oscillations in much shorter loops. This indicates that the damping mechanism of transverse loop oscillations is independent of loop length or period. The displacement profile along the whole length of the oscillating loop is determined for the first time and consistently between *TRACE* and EIT. By comparing the observed profile with models of the three-dimensional geometry of the equilibrium and perturbed loop, we test the effect of longitudinal structuring (spatial seismology) and find that the observations cannot unambiguously distinguish between structuring and non-planarity of the equilibrium loop. Associated intensity variations with a similar periodicity are explained in terms of variations in the line-of-sight column depth. Also, we report intensity oscillations at the loop footpoint, which are in anti-phase with respect to the intensity oscillations in the loop body. Lastly, this observation offers the first opportunity to use the transverse oscillations of the arcade to model the Alfvén speed profile in the global corona.

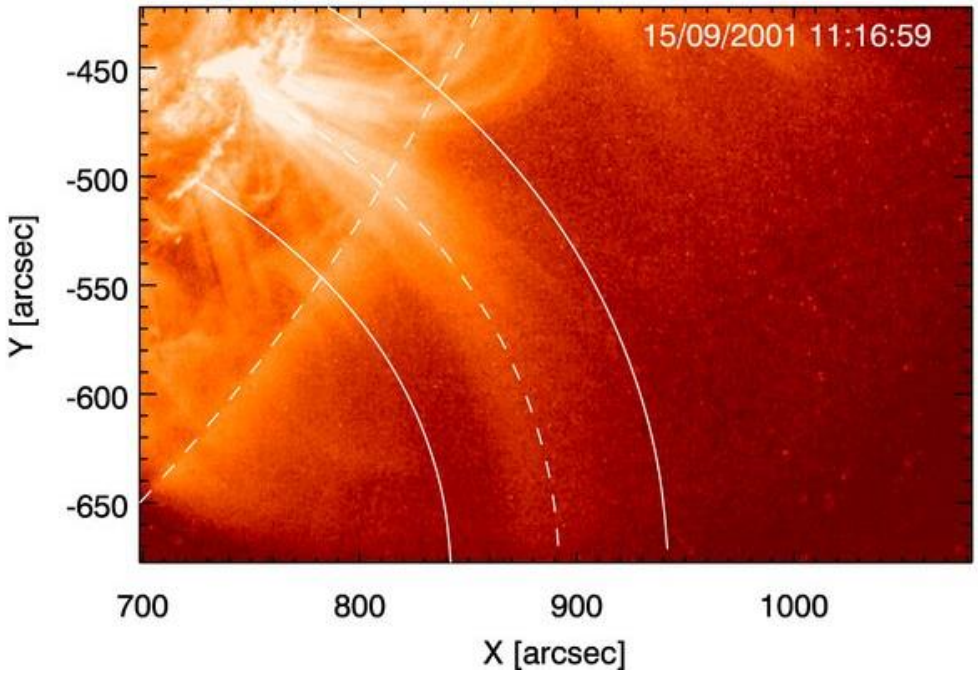

TRACE field of view of the northern leg of the active region loop arcade at 11:17 UT on 2001 September 15. The parallel dashed and solid curves show the central path and width of the loop data cut used, respectively.

Coronal Alfven speed determination: consistency between seismology using AIA/SDO transverse loop oscillations and magnetic extrapolation

Astrophysical Journal, 767, 16 (2013) doi:10.1088/0004-637X/767/1/16

Verwichte, E., Van Doorsselaere, T., Foullon, C. & White, R.S.,

Two transversely oscillating coronal loops are investigated in detail during a flare on the 2011 September 6 using data from the Atmospheric Imaging Assembly (AIA) on board the *Solar Dynamics Observatory*. We compare two independent methods to determine the Alfvén speed inside these loops. Through the period of oscillation and loop length, information about the Alfvén speed inside each loop is deduced seismologically. This is compared with the Alfvén speed profiles deduced from magnetic extrapolation and spectral methods using AIA bandpass. We find that for both loops the two methods are consistent. Also, we find that the average Alfvén speed based on loop travel time is not necessarily a good measure to compare with the seismological result, which explains earlier reported discrepancies. Instead, the effect of density and magnetic stratification on the wave mode has to be taken into account. We discuss the implications of combining seismological, extrapolation, and spectral methods in deducing the physical properties of coronal loops.

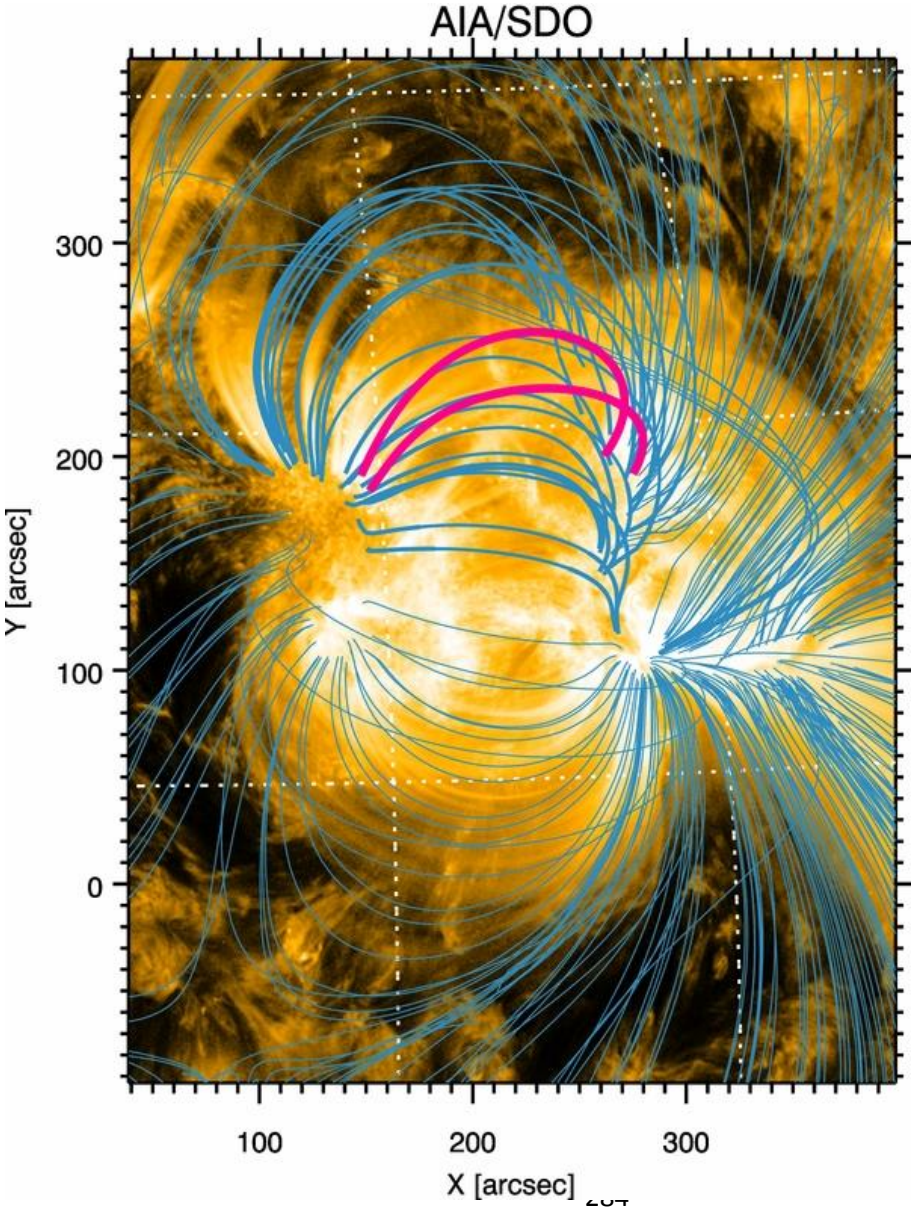

Potential Field Source Surface extrapolation of active region NOAA 11283 on 2011 September 7 at 00:00 UT. The two oscillating loops are indicated in red.

Periodic Spectral Line Asymmetries in Solar Coronal Structures from Slow Magnetoacoustic Waves

Astrophysical Journal Letters 724 (2), L194 (2010) DOI: 10.1088/2041-8205/724/2/L194

Verwichte E., Marsh,M., Foullon, C., Van Doorsselaere, T., De Moortel, I. & Nakariakov, V.M.

Recent spectral observations of upward moving quasi-periodic intensity perturbations in solar coronal structures have shown evidence of periodic line asymmetries near their footpoints. These observations challenge the established interpretation of the intensity perturbations in terms of propagating slow magnetoacoustic waves. We show that slow waves inherently have a bias toward enhancement of emission in the blue wing of the emission line due to in-phase behavior of velocity and density perturbations. We demonstrate that slow waves cause line asymmetries when the emission line is averaged over an oscillation period or when a quasi-static plasma component in the line of sight is included. Therefore, we conclude that slow magnetoacoustic waves remain a valid explanation for the observed quasi-periodic intensity perturbations.

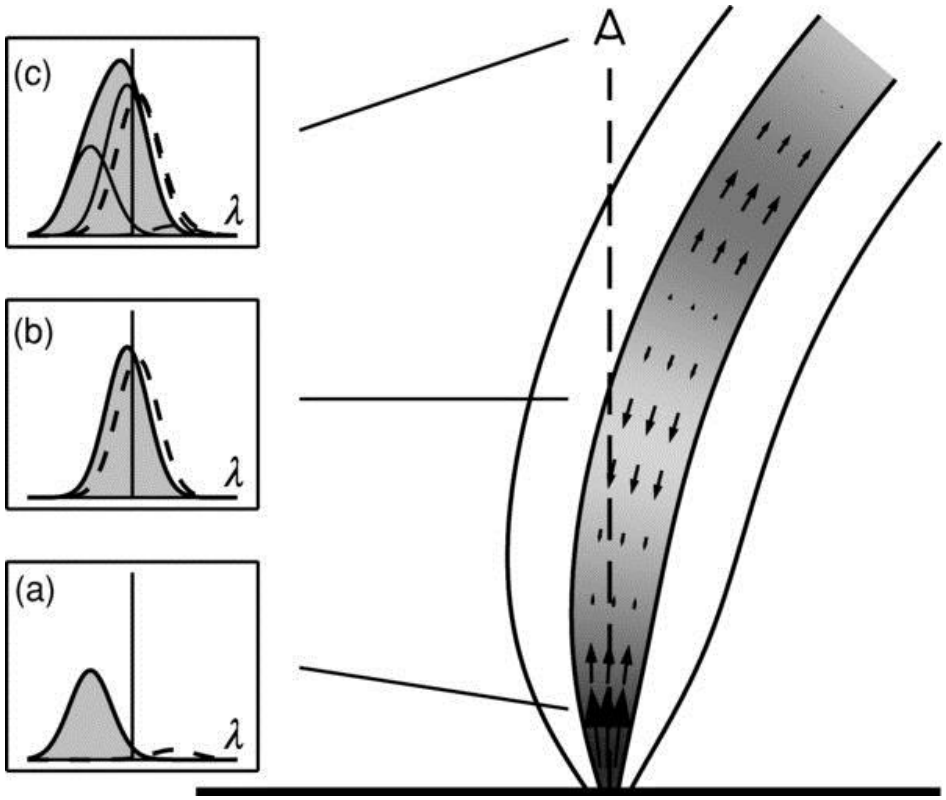

Illustration of the formation of an emission line signature from line-of-sight integration across a loop with a propagating slow wave, whose amplitude may vary with distance from the footpoint, and a static background plasma. The velocity field and intensity perturbation of the slow wave are shown. The inset figures illustrate the emission line at various locations. The solid and dashed curves are for oscillation phase $\phi = 0$ and $\phi = \pi$, respectively. (a) Emission line from the loop with a large amplitude slow wave. (b) Emission line from loop with small amplitude slow wave or from a static background plasma in the line of sight. (c) Total emission line integrated over the line of sight. The thin lines show the two plasma components contributing to the full profile.